

NORMAL FAULT ARCHITECTURE AND SHALE SMEARING AND THEIR
IMPACT ON HYDROCARBON SEALING IN THE NIGER DELTA

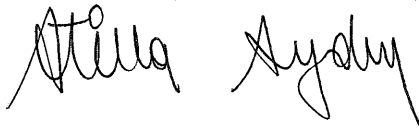
A THESIS

SUBMITTED TO THE DEPARTMENT OF
GEOLOGICAL AND ENVIRONMENTAL SCIENCES
AND THE COMMITTEE ON GRADUATE STUDIES
OF STANFORD UNIVERSITY
IN PARTIAL FULFILMENT OF THE REQUIREMENTS
FOR THE DEGREE OF
MASTER OF SCIENCE

Adeoye Bashir Koledoye

June 1999

I certify that I have read this thesis and that in my opinion, it is fully adequate, in scope and quality, as a thesis for the degree of Master of Science.

A handwritten signature in black ink, appearing to read "Atilla Aydin", written over a horizontal line.

Atilla Aydin, (Adviser)

I certify that I have read this thesis and that in my opinion, it is fully adequate, in scope and quality, as a thesis for the degree of Master of Science.

A handwritten signature in black ink, appearing to read "David D. Pollard", written over a horizontal line.

David D. Pollard (Reader)

Approved for the University Committee on Graduate Studies:

A solid horizontal line intended for a signature.

Abstract

Faults exert significant control on the migration, entrapment and subsequent compartmentalization of hydrocarbon. While some faults allow the passage of fluids across them, others do not, creating varying complications in the geometry of hydrocarbon reservoirs. The current methodology for assessing fault seal integrity ignores important factors controlling the development and growth of faults and the details of the resulting fault zone architecture.

Three-dimensional visualization of a fault from a producing field in the Niger Delta and surrounding stratigraphy, using seismic data, showed that the fault is made up of segments in the dip and strike directions. The fault develops as the separate segments are linked in the strike and dip directions. Wireline log data confirm that the dip segment relay zones act as locations of shale smear. These locations of shale smear are interpreted as barriers for the updip leak of fluids across the fault.

Applying this new understanding of the fault zone architecture, we constructed stratigraphic juxtaposition diagrams with improved resolution. Thus we were able to characterize the lithological composition of the fault zone into areas of shale smear presence and absence using seismic attributes. We then mapped the shale smear in the fault zone across the whole length of the fault. A profile of the initial reservoir fluid pressure gradients on both sides of the fault was used to determine reservoirs sealed or leaking across the fault. The results show a close agreement with our prediction for shale smear distribution.

Acknowledgements

I would like to thank my advisor, Atilla Aydin, for providing much discussion, criticism and insight that greatly improved the quality of work reported here and deeply enriched my understanding of the subject matter. I would also like to thank Dave Pollard for his gentle prodding and encouragement on the theoretical aspects of geomechanics. Eric May helped immensely with discussions and advice on fault geometry and seal analysis, as well as keeping the project on course from the Chevron end.

Chevron Nigeria Limited and the Nigeria National Petroleum Corporation Joint Venture generously funded my studies through a fellowship and provided the data. I am very grateful to all the members of the Nigeria Business Unit of Chevron in San Ramon for their help. Jerome Glass provided invaluable criticism of the shale smear interpretation using well logs. Dave Kissinger helped with moving the seismic data around and keeping the project manageable. Loren Stewart made sure that I got all the log data I needed from San Ramon. Jeff Ortwein helped with engineering data and production information for Okan field. I would also like to express my gratitude to the South Offshore Group in Lagos for their assistance in setting up and maintaining the project. P. C. Okoro and Michelle Ike provided lots of support and discussions on Okan field. Robin Omelagah, Shirley Wilson and Terri Lawrence of the Professional Development Unit of the Nigeria SBU in San Ramon made sure that my family's stay in the States was an enjoyable one. I thank them all.

I thank all the members of the Rock Fracture Project and the Shale Smear Project for providing an environment in which I learnt so much from. Amgad Younes carried out most of the fieldwork in the Gulf of Suez. Our several discussion sessions were very illuminating in understanding shale smear and fault geometry. Laurent Maerten was an invaluable resource in my understanding of fault slip distribution, the FAPS application package and lots of help on the graphics included here. Scott Young was very helpful with suggestion and discussions on normal fault growth and the use of GOCAD. I would also like to express my thanks to my other friends in the School of Earth Sciences, the African Students Association and the Nigeria-Stanford Educational Resources Organization.

Finally, I would like to express my gratitude to my wife, Idayat Dasola, for her unbounded love, patience and loving support throughout the past few years. I couldn't have done this without you. And to my kids, Faridah Adeola and Jamal Adeyanju, for sharing in the familial deprivations occasioned by long stays in front of the workstation away from home.

Table of Contents

Title page.....	i
Signature page.....	ii
Abstract.....	iii
Acknowledgements.....	iv
Table of Contents.....	vi
List of Tables.....	viii
List of Illustrations.....	ix
Introduction.....	1
References for Introduction.....	4
Chapter 1. Three Dimensional Visualization of Normal Fault Segmentation and its Implication for Fault Growth	6
Abstract.....	6
Geological Setting.....	6
Identification of Fault Segments and Shale layers.....	7
Seismic Dip Sections.....	8
Seismic Strike Sections.....	8
Timeslice Views.....	9
Combined View.....	9
Fault Slip Distribution Patterns.....	10
Conceptual Model.....	10
Conclusions.....	11
Suggestions for further reading.....	11

Chapter 2. A Process-based Methodology for the Analysis of Fault Seals Related to Shale Smearing in the Niger Delta.....23

Abstract.....	23
Introduction.....	23
Shale Smearing in the Literature and Practice.....	25
Objectives.....	27
Methodology.....	28
Structural Geology and Stratigraphy.....	29
Conceptual Model.....	30
Mapping Fault Segments on Seismic.....	31
Mapping Smeared Shale With Well Log Data.....	33
Detailed Architecture of Relay Zones.....	34
Seal Analysis Procedure.....	35
Pressure Behavior and its Implication for Seal Integrity.....	37
Sealing Evaluation.....	38
Results and Discussions.....	38
Conclusions.....	40
References.....	59

Appendix A. Shale Smear Analysis Using Well Logs.....62

Introduction.....	62
Algorithms for shale smear quantification.....	63
Methodology.....	63
Mapping smeared shale thickness.....	64
Determining fault throw and slip.....	65
Results and discussion.....	65
Conclusions.....	67
References.....	73

List of Tables

Introduction

(No tables).....

Chapter 1

(No tables).....

Chapter 2

(No tables).....

Appendix A

Table A.1 Measured parameters from the 15 well points, showing calculated fault
 throw and slip.....68

Table A.2 Single, isolated shale source units and their SSR values.....68

List of Illustrations

Chapter 1

- Figure 1.1** Location map of the Okan field and a North-South cross-section of the Niger Delta, showing the tectonic and stratigraphic elements(after Doust and Omatsola, 1989).....13
- Figure 1.2** Project basemap, showing a trace of the fault under study at one of the mapped time horizons, seismic lines and wells from which data was collected.....14
- Figure 1.3** Seismic dip section showing mahor fault segments and wells from which data.....15
- Figure 1.4** Seismic strike section, showing the interaction between two dip fault Segments. Thick shale layers associated with the segments are posted.....16
- Figure 1.5** Timeslice view at 1.8 seconds, showing areal view of two dip segments and the associated thick layer.....17
- Figure 1.6** Conjugate 3-D seismic sections showing the interaction of the different vertical segments of the fault, and the relationship of thick shale layers to the relay zones.....18
- Figure 1.7** Fault slip distribution patterns over two dip segments of Fault X....19
- Figure 1.8** Conceptual model for the development of shale smearing and fault segmentation in the Niger delta.....20

Chapter 2

Figure 2.1	Location map of the Okan field and a North-South cross-section of the Niger Delta, showing the tectonic and stratigraphic elements (after Doust and Omatsola, 1989).....	42
Figure 2.2	Okan megastructure, showing some well projections, some of which cross Fault X.....	43
Figure 2.3a	Idealized normal fault showing shale smearing and associated structures (Weber et al, 1978).....	44
Figure 2.3b	Layered shale smear (Lehner and Pilaar, 1996).....	44
Figure 2.4	Conceptual model for the development of shale smear and dip fault segmentation in the Niger Delta.....	45
Figure 2.5	Okan field basemap, showing trace of Fault X at one of the mapped time horizons.....	46
Figure 2.6	Showing major segments interpreted on seismic dip line 158 and wells providing log data.....	47
Figure 2.7	A section of seismic dip line shown in Figure 2.7, illustrating the spatial relationship between major fault segment relays and thicker shale units.....	48
Figure 2.8	Well log correlation section, showing smeared shale in Well Y as it crosses Fault X between Segments 5 and 6.....	49
Figure 2.9.	Detailed architecture of shale smear interpreted on seismic and well log, using Well Y data.....	50
Figure 2.10	Greater section of Dip line 158, showing detailed architecture of shale smear interpreted on seismic with stratigraphic data from nearby wells.....	51

Figure 2.11	A comparison of the juxtaposition profiles used in this study with that used in conventional analysis.....	52
Figure 2.12	Juxtaposition diagram without fault rock component across Fault X, showing only sands.....	53
Figure 2.13	Areas of sand/sand contact mapped from Figure 2.12.....	54
Figure 2.14	Amplitude distribution on the fault surface, using the proposed juxtaposition profile.....	55
Figure 2.15	Initial bottom-hole pressure profiles for reservoirs in Okan field..	56
Figure 2.16	Sand/sand areas showing pressure depletion status of the different reservoirs in the Footwall block.....	57
Figure 2.17	Modified juxtaposition diagram, incorporating shale smear.....	58

Appendix A

Figure A.1	Relationship between original shale thickness, smeared shale thickness and fault offset.....	69
Figure A.2a	Range of smear intensity recorded in different wells: single shale source.....	70
Figure A.2b	Range of smear intensity recorded in different wells: multiple shale source.....	70
Figure A.2c	Range of smear intensity recorded in different wells: multiple shale source when sand thickness is greater than fault throw.....	70
Figure A.3	Showing measured smeared shale thickness and correction for fault dip.....	71
Figure A.4	Block diagram of Bed X displaced by normal fault, illustrating the different fault components in Table A.1 (modified after Tearpock and Bischke, 1991).....	71

Figure A.5	Normalized shale smear (single unit) vs. normalized fault throw.	
	Throw is on X-axis.....	72
Figure A.6	Normalized shale smear (composite unit) vs. normalized fault throw.	
	Throw is on X-axis.....	72

INTRODUCTION

Faults are important structures in the exploration and production of hydrocarbon because they exert significant control on the migration, entrapment and subsequent compartmentalization of hydrocarbon (Weber, 1978; Akinpelu, 1991). The effect of faults on the flow of hydrocarbon can be complex (Aydin and Eyal, 1995). While some faults allow the passage of fluids across them, others do not, creating varying complications in the geometry of hydrocarbon reservoirs (Weber, 1978; Smith, 1980; Downey, 1984; Akinpelu, 1991; Jev et al, 1993). In order to be able to carry out successful exploration and development of hydrocarbon reservoirs, it is imperative to understand the distribution of hydrocarbon as controlled by sealing faults and the likelihood of production-induced hydrocarbon migration due to the breakdown of these seals.

Those faults that restrict the movement of hydrocarbon are said to be sealed or to act as seals, preventing the movement of hydrocarbon across the fault zone. The sealing action of these faults is with respect to horizontal migration of the hydrocarbon and is distinguished from vertical sealing which is usually caused by caprock (Downey, 1984). The relatively low permeability of these fault zones have been explained by the juxtaposition of lithologies with different permeability values across the fault zone; shale or clay smearing; and fault zone granulation or cataclasis. Several workers have studied the different mechanisms involved in the formation and breakdown of these seals (Weber et al, 1978; Smith, 1980; Downey, 1984; Bouvier et

al, 1989; Akinpelu, 1992; Lindsay et al, 1993; Gibson, 1994; Aydin and Eyal, 1995; Younes and Aydin, 1997).

A methodology for assessing fault seal integrity has evolved as a result of the studies mentioned above. This involves an interpretation of the structural geometry of the field in question and a construction of the stratigraphy of the field and its relationship to structure. It also includes employing special tools like fault slicing and 'Allan maps' to detail stratigraphic juxtaposition across faults, carrying out shale smear analyses; and monitoring changes in reservoir pressure and other production data (Weber et al, 1978; Smith, 1980; Downey, 1984; Bouvier et al, 1989; Akinpelu, 1992; Jev et al, 1993; Gibson, 1994; Eisenberg et al, 1995; Yielding et al, 1996).

However, the process of shale smearing is not well understood yet and there are differences in the methods adopted by different workers in accounting for its contribution to seal integrity (Lehner and Pilaar, 1995; Aydin and Eyal, 1995; Yielding et al, 1996). In addition, constructing juxtaposition diagrams across faults traditionally oversimplifies the fault architecture by assuming a transparent fault zone.

The work reported in this thesis was carried out with the main purpose of developing an improved methodology for the analysis of fault seals in the Niger Delta by increasing the consideration giving to the process of fault development and the resulting fault architecture. The first chapter of this thesis, which is a publication in preparation for The Leading Edge, presents a conceptual model for the development of normal faults in the Niger delta and other areas of clastic deposition using surface and subsurface data. The second chapter, a publication in preparation for The AAPG

Bulletin, presents a fault seal analysis methodology, which uses the fault zone architecture derived from the conceptual model.

Both papers have benefited from discussions and suggestions from many scientists. Atilla Aydin, my adviser, has made enough contribution in both cases that his name will appear as a co-author in the published versions. His contributions were in the form of discussions and advice on the processes of fault development, shale smearing and the architecture of fault zones. Eric May, my mentor in Chevron, made similar contributions, and his name will also appear as co-author in both cases. The author performed all of the seismic interpretation, as well as well log interpretation and correlation.

References

- Akinpelu, O. A., 1991, Faults As Reservoir Seal Project, Internal Report, Chevron Oil Field Research Company, Project Review.
- Akinpelu, O. A., 1992, Faults As Reservoir Seal Project, Internal Report, Chevron Oil Field Research Company, Project Status.
- Allan, A. S., 1989, Model for Hydrocarbon Migration and Entrapment within Faulted Structures: The American Association of Petroleum Geologists Bulletin, 73, P. 803-811.
- Antonellini, M., and A. Aydin, 1995, Effect of Faulting on Fluid Flow in Porous Sandstones: Geometry and Spatial Distribution: The American Association of Petroleum Geologists Bulletin, 79, 642-671.
- Bouvier, J. D., K. Sijpesteijn, D. F. Kluesner, C. C. Onyejekwe, and R. C. Van der Pal, 1989, Three-dimensional Seismic Interpretation and Fault Sealing Investigations, Nun river Field, Nigeria: The American Association of Petroleum Geologists Bulletin, 73, 1397-1414.
- Crans, W., G. Mandl and J. Haremboure, 1980, On the Theory Of Growth Faulting: A Geomechanical Delta Model Based On Gravity Sliding: Journal of Petroleum Geology, 2, 3, 265-307.
- Downey, M. W., 1984, Evaluating Seals for Hydrocarbon Accumulations: The American Association of Petroleum Geologists Bulletin, 68, 1752-1763.
- Eisenberg, R. A., R. J. Brenneman, A. A. Adeogba, and U. K. Acharaya, 1996, Integrated Fault Seal Analysis, Risk Management and Reservoir Management: Okan Meren Fields, Nigeria: Book of Abstracts-conference on Faulting, Fault Sealing and Fluid Flow in Hydrocarbon Reservoirs, Rock Fracture Deformation Research, University of Leeds.
- Evamy, B. D., J. Haremboure, P. Kamerling, W. A. Knaap, F. A. Molloy, and P. H. Rowlands, 1978, Hydrocarbon Habitat of Tertiary Niger Delta: The American Association of Petroleum Geologists Bulletin, 62, 1-39.
- Gibson, R. G., 1994 Fault-zone Seals in Siliciclastic Strata of the Columbus Basin, Offshore Trinidad: The American Association of Petroleum Geologists Bulletin, 78, 1372-1385.
- Jev, B. I., C. H. Kaars-Sijpesteijn, M. P. A. M. Peters, N. L. Watts and J. T. Wilkie, Akaso Field, Nigeria: Use of 3-D Seismic, Fault Slicing, Clay Smearing and RFT Pressure Data on Fault trapping and Dynamic Leakage, : The American Association of Petroleum Geologists Bulletin, 77, 1389-1404.

- Lehner, F. K. and W. F. Pilaar, The Emplacement of Clay Smears in Synsedimentary Normal Faults. Inferences from Field Observations near Frechen, Germany - unreferenced.
- Lindsay, N. G., F. C. Murphy, J. J. Walsh, and J. Watterson, 1993, Outcrop Studies of Shale Smears on Fault Surfaces, Spec. Publs. Int. Ass. Sediment, 15, 113-123.
- Short, K. C. and Stauble, A. J., 1967, Outline of Geology of Niger Delta: The American Association of Petroleum Geologists Bulletin, 51, 761-779.
- Smith, D. A., 1966, Theoretical consideration of Sealing and Non-sealing Faults: : The American Association of Petroleum Geologists Bulletin, 50, 363-374.
- Smith, D. A., 1980, Sealing and Non-sealing Faults in Louisiana Gulf Coast Salt Basin: The American Association of Petroleum Geologists Bulletin, 64, 145-172.
- Weber, K. J., and E. Daukoru, 1975, Petroleum geology of the Niger Delta: Ninth World Petroleum Congress transactions, 2, 209-221.
- Weber, K. J., G. Mandl, W. F. Pilaar, F. lehner, and R. G. Precious, 1978, the role of Faults in Hydrocarbon Migration and Trapping in Nigerian Growth Structures, In Tenth Annual Offshore Conference Proceedings, 4, 2643-2653.
- Weber, K. J., 1987, Hydrocarbon Distribution Patterns in Nigerian Growth Fault Structures Controlled by Structural Style and Stratigraphy: Journal of Petroleum Science and Engineering, 1, 91-104.
- Yielding, G., B. Freeman and T. Needham, 1996, In-situ Calibration of Algorithms for Fault-seal Prediction: Book of Abstracts- Conference on Faulting, Fault Sealing and Fluid Flow in Hydrocarbon Reservoirs, Rock Fracture Deformation Research, University of Leeds.

Three Dimensional Visualization of Normal Fault Segmentation and its Implication for Fault Growth

Abstract

Segmentation is a fundamental feature of faults that has been reported for all kinds of faults at different scales. It has significant impacts on hydrocarbon migration and flow for transmitting faults and on reservoir fluid estimates and compartmentalization for sealing faults. In spite of these great benefits, applications of the knowledge of fault segmentation to hydrocarbon exploration and production is rather limited due sometimes to poor seismic data quality and resolution and sometimes to the lack of understanding of how this knowledge can be utilized. We present here an example for a three-dimensional segmentation of a normal fault in the Niger Delta and a methodology to visualize fault segments and their slip distribution patterns using seismic and well data.

Geological Setting.

The data-set used in this study includes a reprocessed full-fold 3D seismic survey from offshore Niger Delta and well data from a developed oil field, the Okan field, in the same basin (Figures 1.1 and 1.2). The study focused on one fault system (Fault X) that has excellent seismic images and numerous wireline logs from wells crossing it (Figure 1.2).

The Niger Delta has been subdivided into three broad lithofacies units which include massive continental sandstones (Benin formation), paralic sandstones, shales

and clays (Agbada formation), and marine shales (Akata formation). This generally regressive clastic sequence reaches a maximum thickness of between 9km to 12 km (Figure 1.1). The structural development of the Niger delta since the Middle Eocene has been dominated by growth faulting and associated rollovers in the shelf portion. Beyond the shelf break, the sequence becomes compressive. Structural analysis of the Tertiary overburden shows that individual fault blocks can be grouped into macrostructural and eventually megastructural units. Such megastructural units are separate provinces with regard to time-stratigraphy, sedimentation, deformation, generation and migration of hydrocarbons as well as hydrocarbon distribution. The Okan field is an example of a megastructure and the sand and shale sequence involved is of Middle Miocene to Lower Pliocene in age.

Identification of fault segments and shale layers.

The fault segments were identified on the seismic dip lines primarily by the distinct discontinuity of seismic characters on either side (Figure 1.3). The mapping process enabled us to delineate the fault segments with an en echelon arrangement in the dip direction. Next shale layers in the succession were identified in order to establish their geometrical relationship with the fault segments already interpreted on the seismic sections. Using the best velocity profile for each well, gamma ray and resistivity curves were posted on the seismic dip sections. Lithology data from wireline logs of wells in the field were then posted to establish the vertical locations of the shale units thicker than twenty feet. A paper in preparation for the AAPG Bulletin discusses in detail the relationship between the fault segments, neighboring

shale units and fault rock made up of smeared shale. Preliminary mapping of the fault segments was done on a spacing of every eight dip lines and every sixteen strike lines. The horizon mapping and fault interpretation exercises were alternatively iterated later at closer intervals of two dip lines to four strike lines. A synthetic seismogram was also created to confirm the lithologies associated with the seismic characters.

Seismic Dip Sections.

The Inline seismic sections provide the easiest means to view the vertical segmentation of the fault. The sections show the fault under study being made up of fourteen different segments having varying heights, overlaps with neighboring segments and separations. The segments show a consistent left-stepping relay geometry (Figure 1.3). The overlaps are greater, but thinner, along the deeper segments, with higher slip magnitudes. The overlaps reduce along the shallower segments, which become well separated, with lesser slip magnitudes and nearly underlap at the very top.

Seismic Strike Sections.

The Crossline sections permit the identification of the dip segments along strike (Figure 1.4) and the strike variation in the geometry of the relay zones established from the Inline sections. It is more difficult however, based on these sections alone, to discern the existence of segmentation of the fault in the strike

direction. This difficulty arises from the fact that the original strike segments have already linked, producing a long and continuous fault trace. Also, the changing orientation of the fault along strike due to a scoop like three-dimensional geometry of the fault does not help. However, the use of slip distribution patterns along the fault surface helps to determine heterogeneous slip distribution with more than one maxima, which indicates the existence of fault segment linkage along strike. We show the result of this application later in the report.

Timeslice Views.

The timeslices afford an areal view of the fault segments, principally indicating the strike of the segments. It allows for the detection of the time range of occurrence of the relay zone, with its corresponding strike correlation. The slice view also shows the overlaps of the segments that are next to each other (Figure 1.5).

Combined View.

Creating a cube with conjugate seismic sections (Figure 1.6) enables us to better appreciate the three-dimensional geometry of the fault and the relay zones. The cube illustrates the fault segmentation in three dimensions and how the along-dip segmentation is related to major shale horizons. Also, it is clear from this visualization that fault segments are three-dimensional structures with straight cross-sectional traces, but highly curved map traces.

Fault Slip Distribution Patterns.

We have used the pattern of vertical component of slip distribution for the fault under study to further understand the process of fault development. In each of the following illustrations, the earth surface is towards the top of the page. Figure 1.7a, shows slip distribution patterns over one dip segment (Segment 5 in Figure 1.3). Figure 1.7b, shows the patterns over the lower neighboring segment (Segment 4). The slip distribution magnitudes were determined by taking offset values on seismic horizons on either side of the fault segments.

Although the patterns do not fully represent the tipline of each segment, they indicate certain features related to the fault growth and development. Figure 1.7a shows two separate slip maxima in the middle, indicating that there might have been separate segments in the strike direction, which later linked up. The longitudinal pattern of slip reduction at the base of the zone of overlap between the two segments (Figure 1.7c) indicates the presence of a relay zone between the two segments.

Conceptual Model.

In the Niger delta and similar environments, the depositional sequence is made up of alternations of sands and shales. The resulting contrast in the mechanical properties of these lithologic types results in a significant difference in their reaction to deformation. The sandstones react under gravity by brittle deformation, while the shales react by ductile deformation. This leads to the termination of fault segments at sand/shale boundaries and consequently, the abrupt separation of sandstone layers across the fault, but thinning and stretching of the ductile shale layers through the

fault zone as illustrated by schematic diagrams in Figure 8. Once incorporated into the relay zones, the shale lithology is referred to as a 'smear'. The original thickness of the corresponding shale in the stratigraphic section and the magnitude of slip control the thickness of the smeared shale. At a critical point, the continuity of this shale body in the relay zone is broken, leading to the linkage of the adjacent dip segments. The fault segmentation in the dip direction is clearly visible on Inline sections of the seismic data examined from the Niger Delta (Figure 3).

Conclusions.

Well data and 3-D seismic data have been used to evaluate the three-dimensional geometry of a fault in the Niger Delta and the associated shale smearing. The fault zone appears to be made up of several discontinuous segments in both dip and strike directions. Along dip, segmentation is believed to result from vertical mechanical anisotropy between alternating ductile shale and brittle sand units. As such, the segments initiate in brittle sand units and terminate in ductile shale units. The vertical propagation of such a system would produce consistently left-stepping segments whose relay zones are the locations of smeared shale units. Such fault zones represent areas of enhanced lateral sealing potential. Segmentation in the strike direction is probably caused by the initiation and growth of the faulting process at multiple locations in brittle sand units. In contrast to segmentation in the dip direction, there is no impediment to fault linkage along strike within the sand units. Eventually these segments mechanically interact and link, forming longer composite faults with greater lengths and shorter heights.

Given this fault geometry in three dimensions, migration and entrapment of hydrocarbon will depend on the timing of the merging of the fault segments in the strike direction, as well as the dynamics of the formation of the shale smear within the relay zones in the dip and strike directions

The approach outlined above demonstrates how knowledge of fault formation and propagation can be used to interpret fault segmentation and fault rock in a sand/shale sequence with the aid of seismic and well log data.

Suggestions for further reading:

The visualization of fault rock within this fault zone is the subject of a more detailed manuscript to be submitted to the AAPG Bulletin by the same authors.

Willemse (1997) and Crider and Pollard (1998) discuss segmented geometry of normal faults and interaction between neighboring fault segments. Aydin and Nur (1986) also discuss fault segmentation in three dimensions.

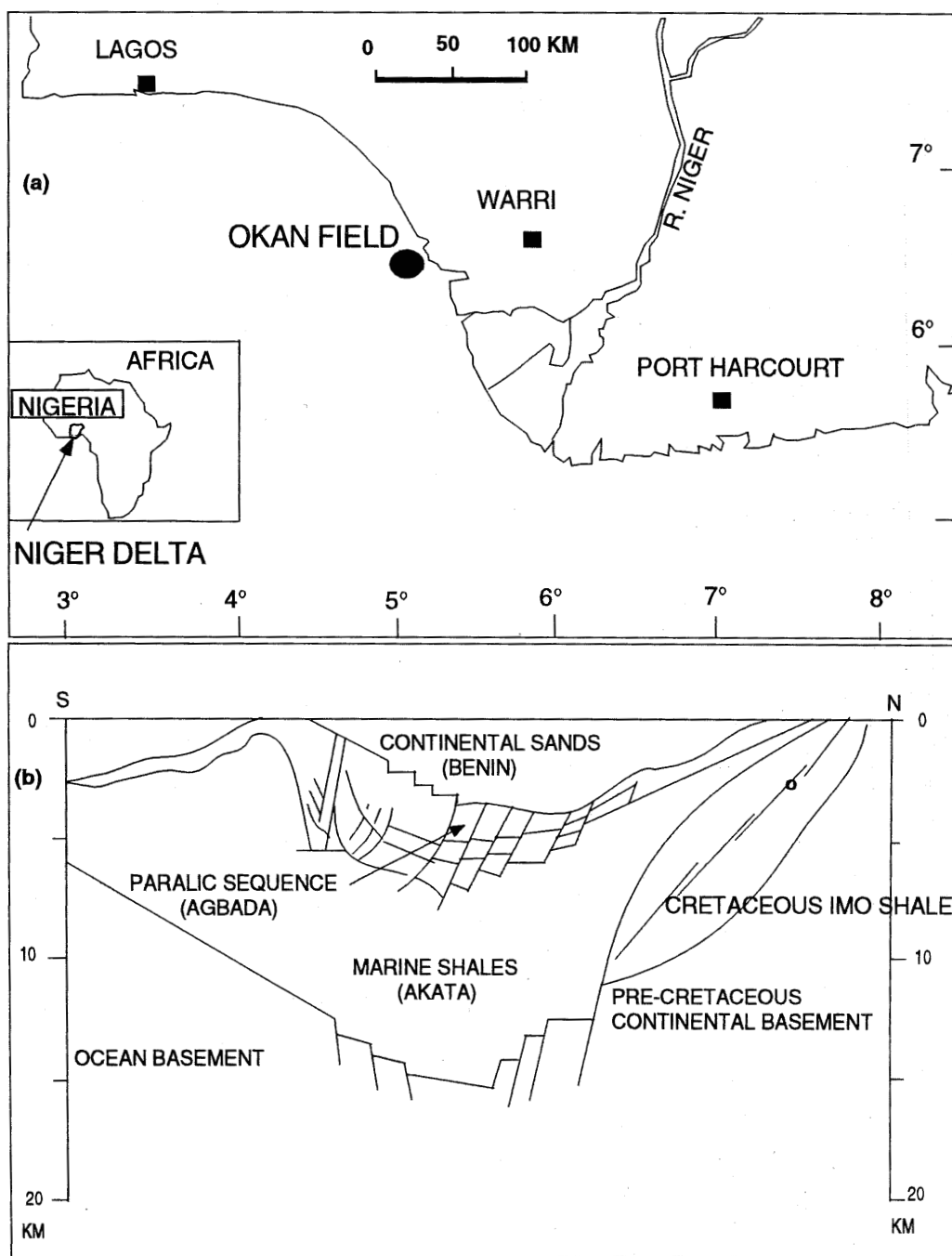


Figure 1.1: (a) Location map of the Okan field and (b) a North-South Crosssection of the Niger Delta, showing tectonic and stratigraphic elements (after Doust and Omatsola, 1989).

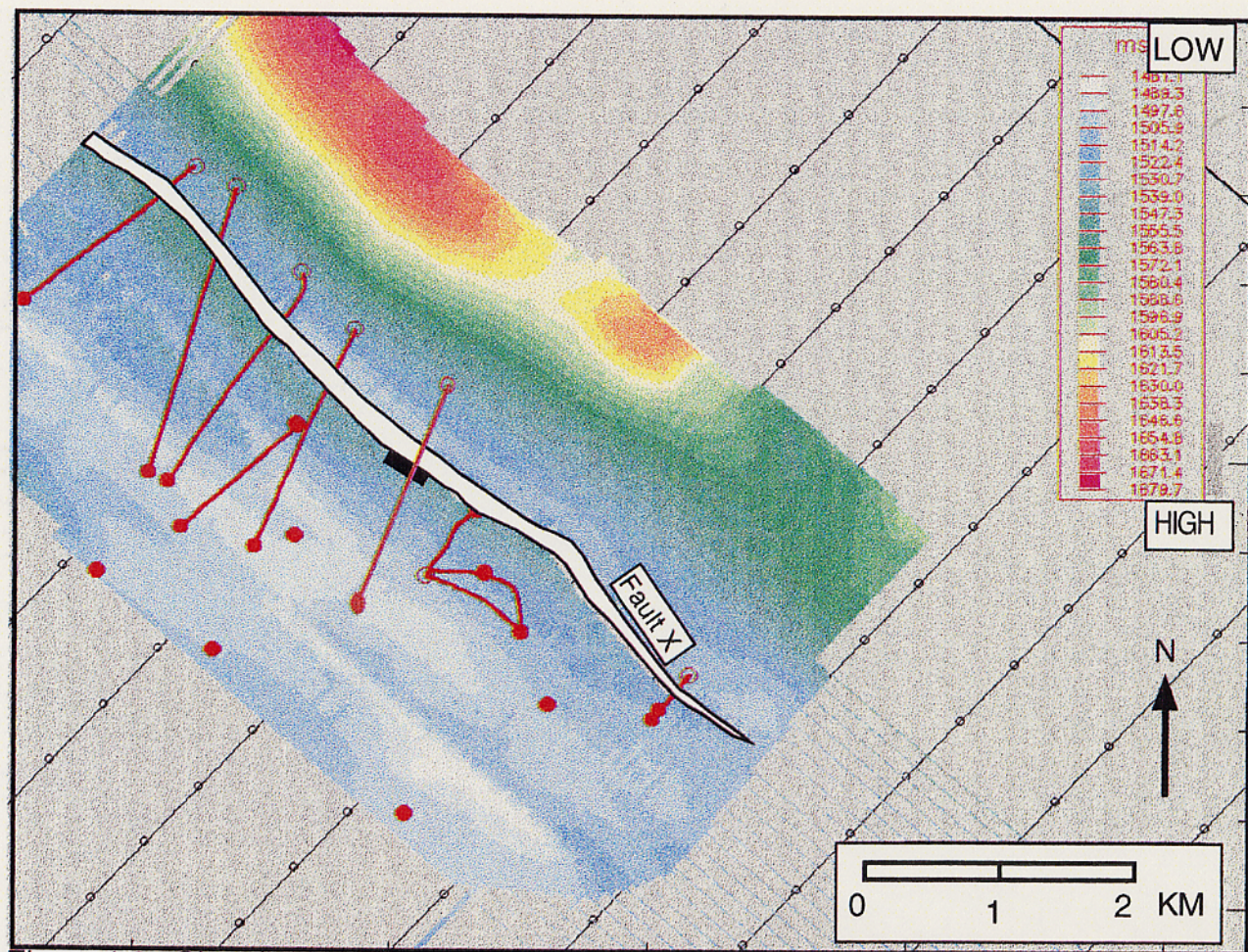


Figure 1.2: Okan field basemap, showing trace of Fault X at one of the mapped time horizons. The red lines are directional wells while the red points are straight vertical wells. The fault dips to the southwest. Notice many of the wells crossing the fault.

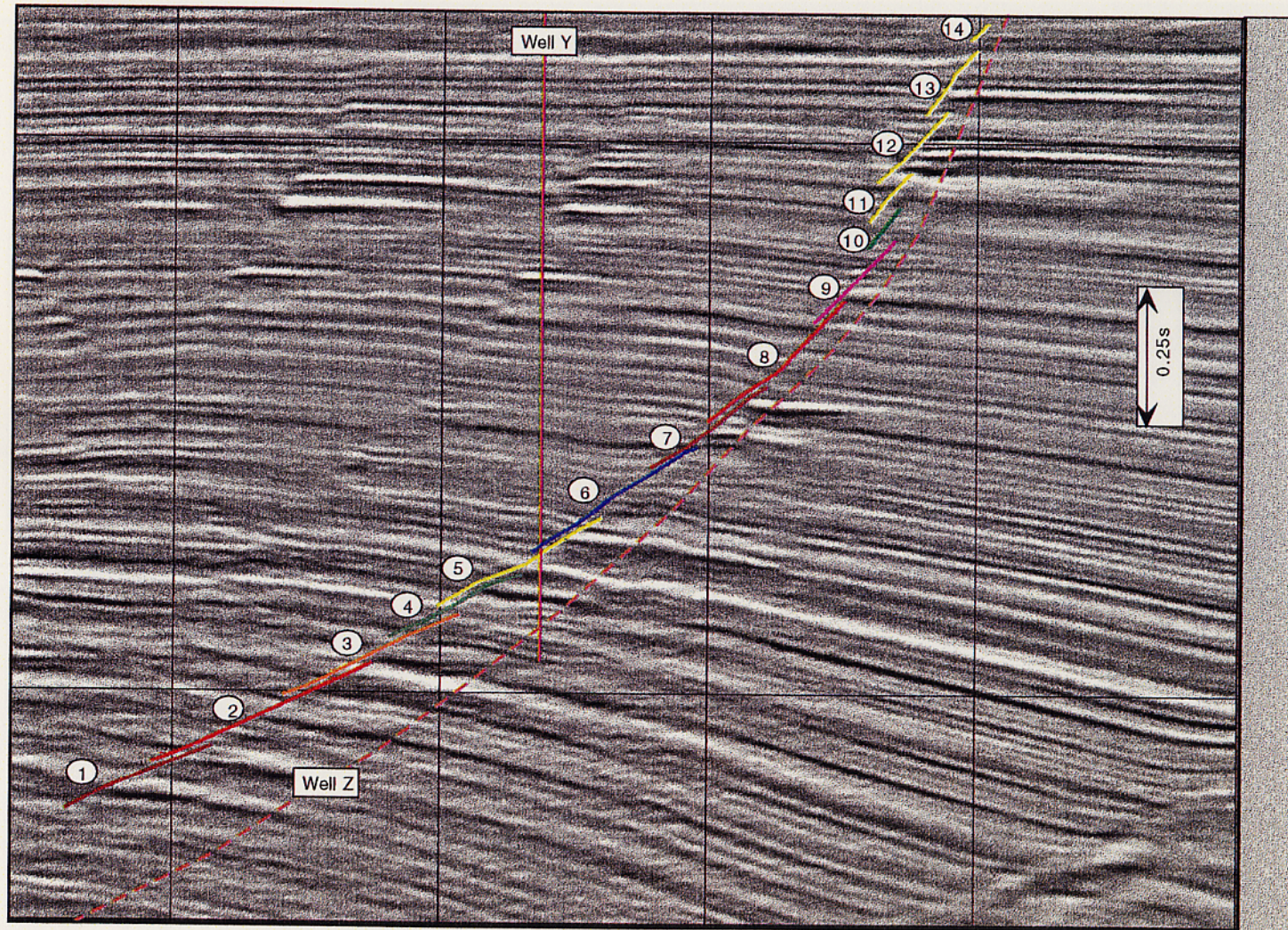


Figure 1.3: Showing major fault segments interpreted on seismic dip line and wells providing log data. The segments are numbered from 1 at the base to 14 at the top. Note how the relay width and segment overlap areas vary systematically from base to top.

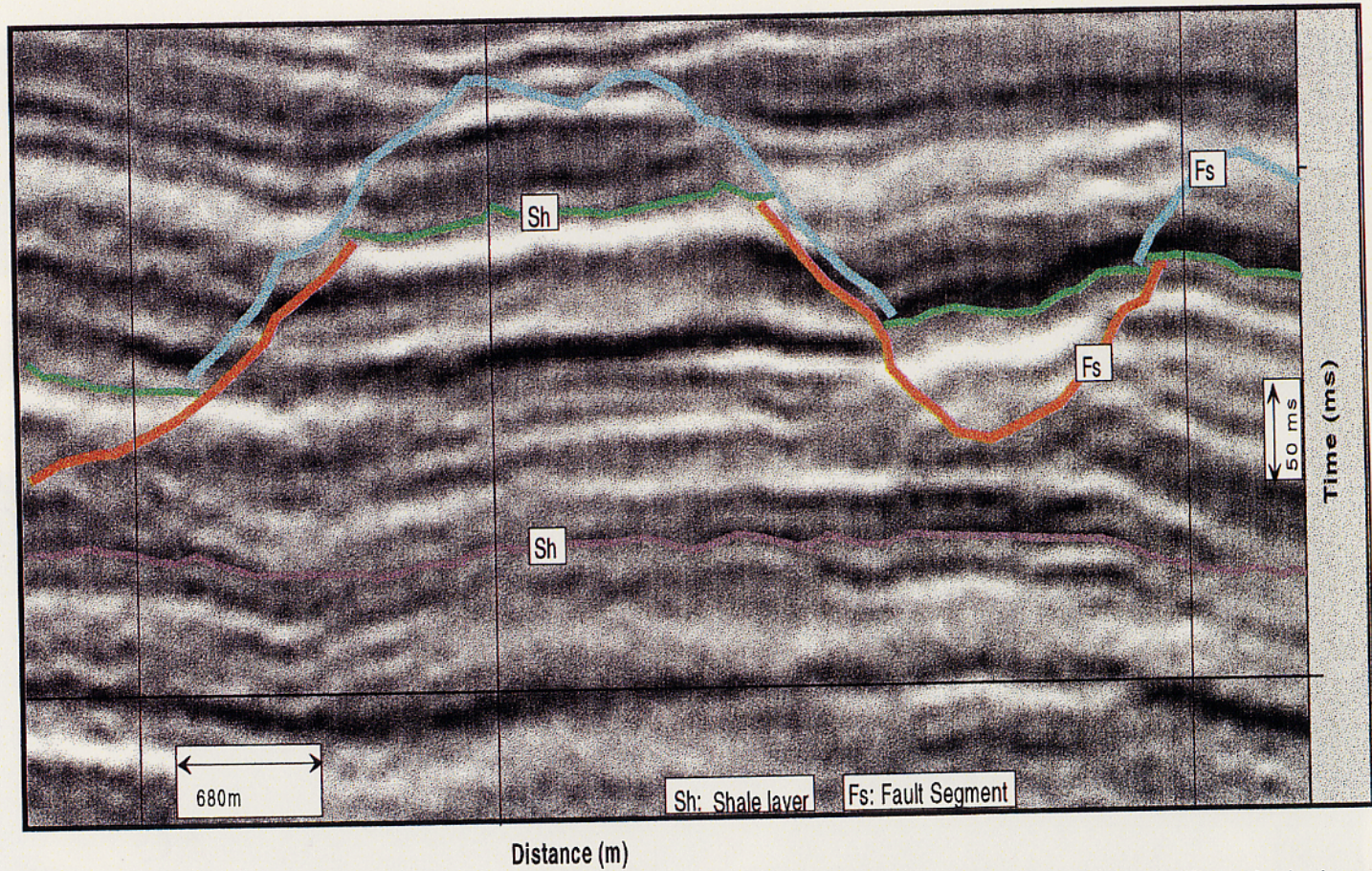


Figure 1.4: Seismic Strike Section, showing the interaction between two dip segments. The shale layers associated with them are posted, using the same color scheme as in Figure 1.3

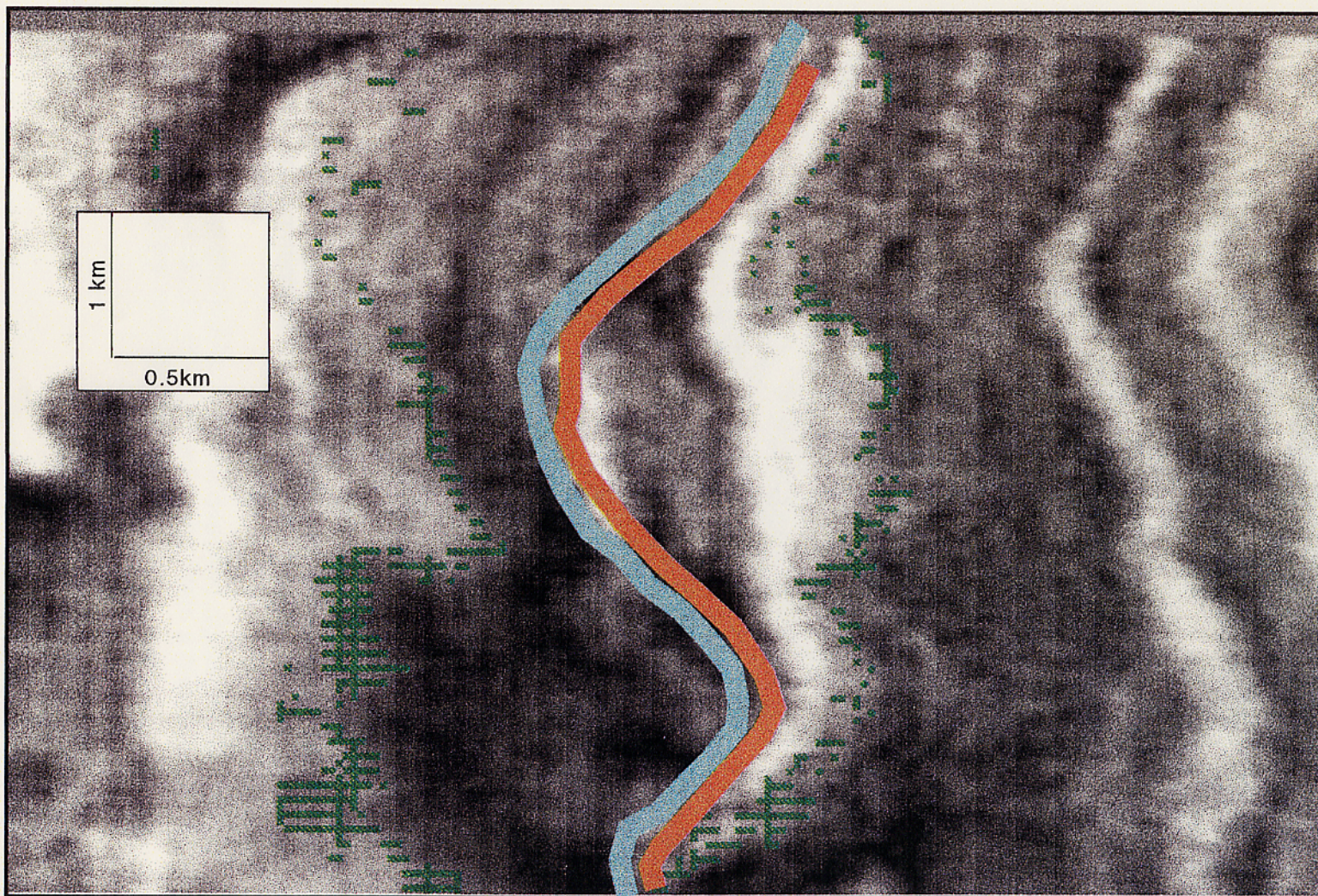


Figure 1.5: Timeslice section at 1.8 seconds, showing areal views of two dip fault segments and the associated thick shale layer. The color scheme is the same as in Figure 1.3. Note that it is possible to see the two dip segments at this time instance over some distance.

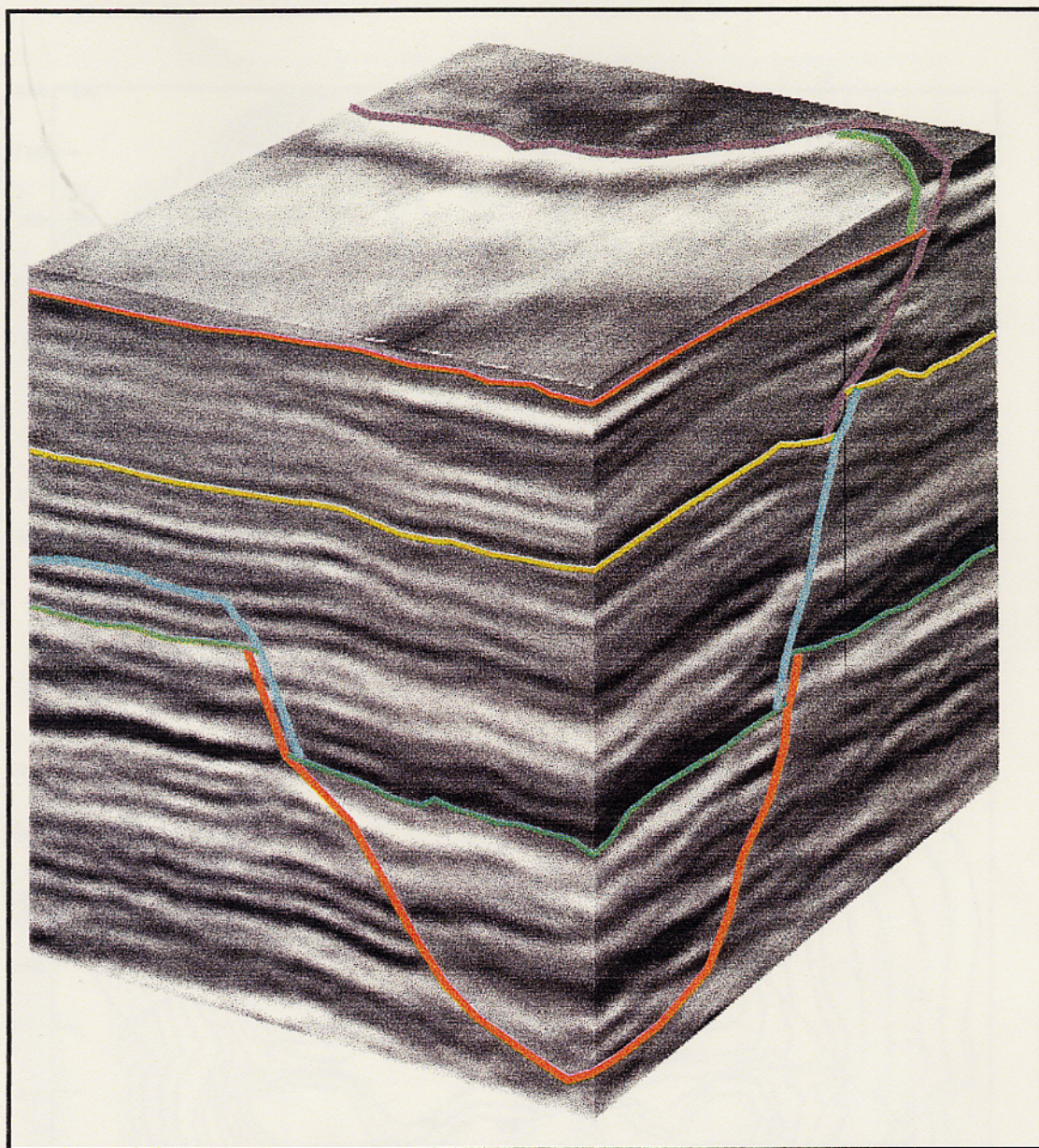


Figure 1.6: Conjugate 3-D seismic sections showing the interaction of the different dip segments of the fault, and the relationship of thickshale layers to the relay zones.

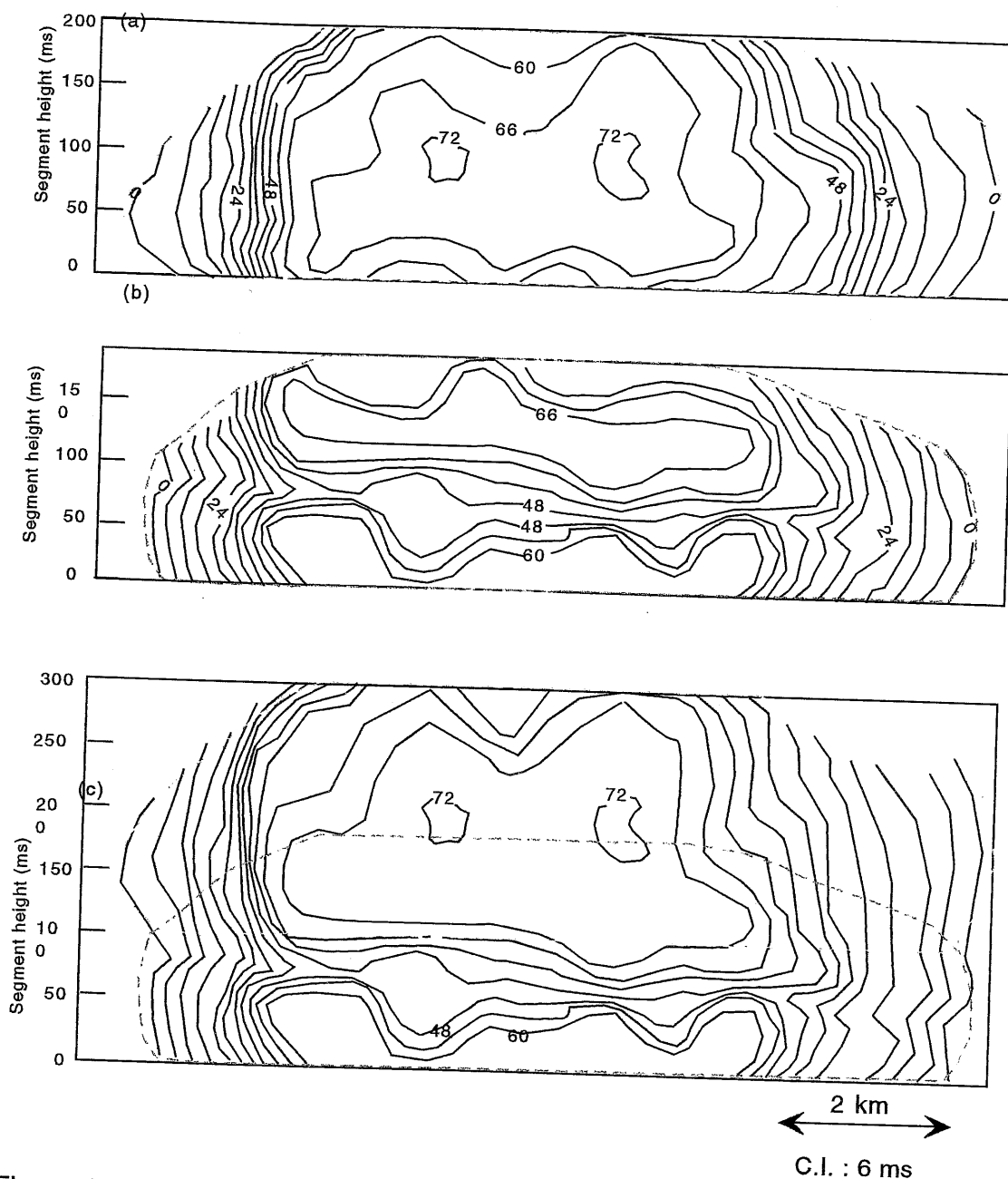
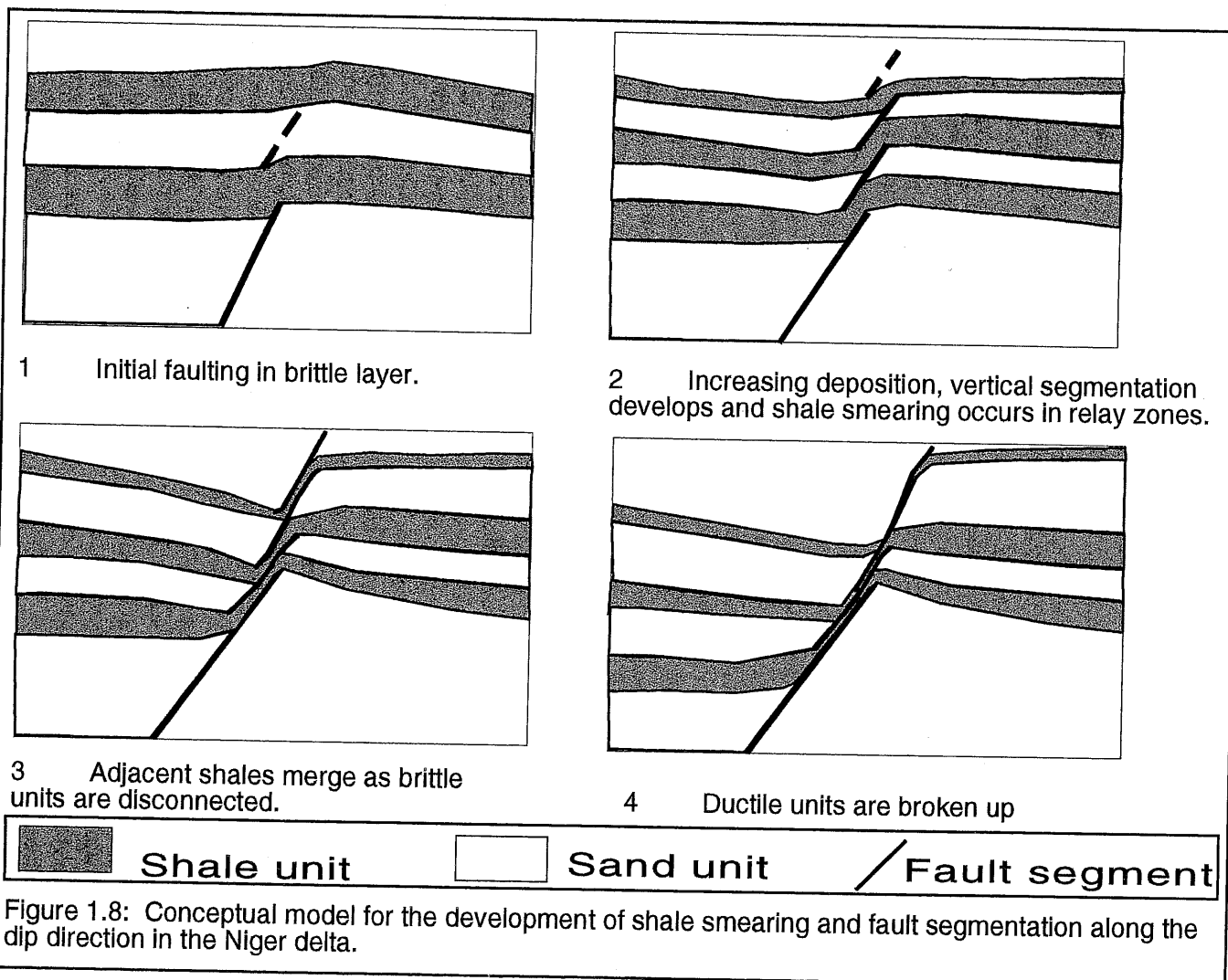


Figure 1.7 Fault slip distribution patterns over two dip segments of Fault X. (a) From Segment 5. (b) From Segment 4. (c) From a combination of both segments, showing the overlap zone



A NEW, PROCESS-BASED METHODOLOGY FOR THE ANALYSIS OF FAULT SEALS IN THE NIGER DELTA

ABSTRACT

3D seismic and well log data from the producing Okan field in the Niger Delta and a working conceptual model derived from field observations and theoretical considerations were used to map the three dimensional geometry of a representative normal fault with shale smear. Seismic data show clear fault segmentation in the dip direction with extensional relays occupied by smeared shales. Log data help to identify lithologic horizons throughout the field and in some cases, where the wellbores crossed the fault, to quantitatively determine the amount of smeared shale within the fault zone. Conceptual models provide means to interpret crucial details of the fault geometry and the distribution of fault rock beyond the conventional resolution of a 3D seismic data set.

Combining these three approaches, we have developed a procedure to determine the fault geometry and to assess the nature of the smeared shales and their evolving configurations as a function of fault throw and the thickness of corresponding shale units. The result is a new and improved technique to visualize fault architecture and to interpret fault rock, both of which lead to constructing structurally realistic juxtaposition diagrams and physically sound fault seal analyses in reservoirs.

INTRODUCTION

Faults are important structures in the exploration and production of hydrocarbon because they exert significant control on the migration, entrapment and

subsequent compartmentalization of hydrocarbon (Weber, 1978; Smith, 1980; Downey, 1984). The effect of faults on the flow of hydrocarbon can be complex: while some faults allow fluid flow across them, others do not (Aydin, 1999), causing various complications in the geometry of hydrocarbon reservoirs. In order to improve the efficiency in exploration and development of hydrocarbon reservoirs, it is imperative to understand the distribution of faults and their internal architecture and petrophysical property.

The impacts of faults on hydrocarbon flow are two-fold: First major effect is the juxtaposition of stratigraphy across the fault and second is the nature of the fault rock. Two most common processes responsible for different fault rocks are shale or clay smearing and granulation or cataclasis. The relatively low permeability of the sealing faults in the Niger Delta has been attributed to the juxtaposition of lithologic units with low permeability values against reservoirs across the fault zone and shale smearing (Eisenberg et al, 1996; Bouvier et al, 1989; Weber, 1987; Weber et al, 1978). A limited number of other workers studied the formation and breakdown of fault seals by shale smearing (Smith, 1980; Downey, 1984; Lindsay et al, 1993; Gibson, 1994; Yielding et al, 1997; Lehner and Pilaar, 1997; Aydin and Eyal, 1999; Younes and Aydin, 1999).

Mapping the juxtaposition of stratigraphic units across the fault plane is sufficient to characterize juxtaposition seal. Accurate fault geometry and the nature and distribution of smeared shale are required for a sound assessment of fault seal due to fault rock. However, the interdependence of the two mechanisms poses a challenge in applications: the juxtaposition geometry is strongly controlled by the

distribution of the fault rock along a fault zone. Therefore, we submit that a reliable seal analysis will first require an accurate map of fault geometry and fault rock within a fault zone.

In this paper, we present a new methodology based on 3D seismic, wireline logs and conceptual models of faulting in brittle/ductile multilayers to analyze fault seals from Okan field, one of the largest producing fields in the Niger Delta (Figures 2.1 and 2.2). We argue that unlike current methodologies, this procedure follows closely the principles of the process of shale smearing and provides means of visualizing fault architecture in a detail that wasn't possible before. In turn, this improvement makes it possible to construct a more accurate juxtaposition diagrams, which should form a basis for a physically sound fault seal analysis.

SHALE SMEARING IN THE LITERATURE AND PRACTICE

The observations presented by Weber et al (1978) have provided a good understanding of shale smearing developed in unlithified sequences, named 'shear smears'. Their presentation included observations from experiments and outcrop studies. Lehner and Pilaar (1997) later expanded the outcrop study at the same locality and its empirical results. They showed that fault displacement along the major normal faults was partitioned over a number of slip surfaces defining a 'shear zone'. Such shear zones often have a lithologically stratified appearance, containing smeared shale in almost every location within the throw interval of a faulted shale bed (Figures 2.3a,b).

Lindsay et al (1993) reported an outcrop study of shale smear in tectonic faults developed within lithified sequences and identified a number of different

mechanisms for the development of shale smear including: 1.) 'Abrasion smears', comprising a shale veneer that is abraded by a sandstone wallrock as it slips past a shale bed; 2.) 'Shear smears'; analogous to those described by Weber et al. (1978) as mentioned above; and 3.) 'Injection smears', which are a local response to volume changes during faulting.

A number of field based studies have been carried out at the Stanford Shale Smear Project for the purpose of characterizing shale smearing along large scale faults and defining the critical point at which smeared shale breakdown (Aydin and Eyal, 1999; Younes and Aydin, 1999). They concluded that smeared shale thickness depends on the original thickness of the shale bed and the magnitude of the normal slip. Gibson (1994), Aydin and Eyal (1999), and Younes and Aydin, 1999) suggested that smeared shale vanishes above a slip/shale bed thickness ratio between 4 and 6.

Other workers have proposed shale smear analyses using primarily subsurface data. The general conclusions from these studies are: (1) thicker source beds produce thicker shale smears, (2) shear-type smears decrease in thickness with distance from the source layer; (3) relative smearing potential increases with the number of source beds passing a point on the fault plane (Yielding et al, 1997). Based on the factors mentioned above, a number of algorithms are being used in practice that seek to quantify the smear values at particular points along the fault zone in the subsurface. Yielding et al (1997) provide an excellent discussion on the different algorithms currently used for shale smear analysis. For

example, the Shale Gouge Ratio (SGR) is defined as ‘the percentage of shale or clay in the slipped interval’. To calculate the SGR at a given point on a fault surface, for discrete shale beds the equation,

$$\text{SGR} = \frac{\text{(Shale bed thickness)}}{\text{Fault throw}} \times 100\%,$$

is used. To use the algorithms as estimates of seal capacity, they must be calibrated in data sets where sealing behavior is documented from production data.

The other algorithms also consider similar variables. As such, they are only indirect estimates of shale smear being developed at the fault surface. Lehner and Pilaar (1997), while noting that the length of continuous smears will ultimately be controlled by the smearing process, remind us that the process itself is yet to be investigated in detail.

The most significant defect in the current algorithms remains that they are not really based on the process of fault development or shale smearing. Rather, they are basically empirical ranking procedures that rely very largely on the geometric relationships between lithologic sequences and fault offsets in a stochastic manner. Because of the shortcomings inherent in using the statistical methodology described above, we decided to further investigate the processes of shale smearing and thereby seek ways to improve the quantitative analysis of shale smear and its consequent effect on fault seal.

OBJECTIVES

The objectives of the present study are

1. To determine the physical factors controlling the shale smearing process and develop a conceptual model for their formation and development.
2. To interpret the subsurface data in Okan field in the light of our conceptual understanding of faulting in multilayered brittle/ductile sequences.
3. To determine which of the factors contributing to the shale smearing process could be directly related to the fault sealing
4. To compare the results to those from similar studies.

METHODOLOGY

In this study we have used 3D seismic, wireline logs, and conceptual models of faulting in layered elastic/plastic medium. The procedure adopted to achieve our objectives are listed below:

1. Use field observations and theoretical considerations to develop a conceptual model for the formation and evolution of shale smearing within faults in the Niger Delta.
2. Produce a rigorous interpretation, in three dimensions, of the geometry of the fault under study in light of the conceptual model.
3. Use well log data to identify and map reservoir and non-reservoir stratigraphy associated with the fault. Compare the data to the conceptual model.
4. Conduct a detailed investigation of the architecture of fault zones and the fault rock.

5. Map the distribution of fault rock (due to shale smear) across the fault surface and construct a physically realistic juxtaposition diagram.
6. Use pressure data to validate the sealing characteristics of the fault in the producing field.

STRUCTURAL GEOLOGY AND STRATIGRAPHY

The structural development of the Niger Delta since the Middle Eocene has been dominated by growth faulting and associated rollovers (Short and Stauble, 1967). According to Akinpelu (1991), it is conceivable that the ductile Imo shale and the subsequent offshore equivalent, the Akata shale, could be an initial surface of detachment on which the growth fault tectonics of the Niger Delta hinged (Figure 1). Structural analysis of the Tertiary overburden shows that individual fault blocks can be grouped into macrostructural and eventually megastructural units. Megaunits are separate provinces with regard to time-stratigraphy, sedimentation, deformation, generation and migration of hydrocarbons as well as hydrocarbon distribution (Evamy et al, 1978). The Okan field is an example of such a megastructure (Figure 2.2).

The Niger Delta has been subdivided into three broad lithofacies units which include massive continental sandstones (Benin formation), paralic sandstones, shales and clays (Agbada formation), as well as marine shales (Akata formation) (Bouvier et al, 1989). This generally regressive clastic sequence reaches a maximum thickness of between 9km to 12 km (Figure 2.1).

Fault X, the fault under study, divides the Okan field into roughly two producing blocks (Figures 2.2 and 2.5). The hanging wall comprises of wells mostly drilled in the 1960's to the 1980's, while the foot wall comprises of wells drilled in the late 1980's and the 1990's.

CONCEPTUAL MODEL

In the Niger Delta and similar environments, the depositional sequence is made up of alternating sands and shales. The resulting contrast in the mechanical properties of these lithologic rock types leads to differences in their reaction to deformation. It is proposed that the shale layers generate segmentation in the dip direction of normal faults as described below.

The sandstones react under gravity by brittle deformation, while the shales react by ductile deformation. This will lead to abrupt discrete separation of the fault segments within brittle sandstone layers, but a distributed zone of deformation in the shale layers (Figure 2.4A). Note that regardless of the propagation direction, fault growth from the top or from the base would result in steps in the sense that the top segment is located to the left of the bottom segment. This corresponds to a series of extensional relay structures in which smeared shale layers deform by thinning and stretching (Figure 2.4B). If the shale layer is thick enough with respect to the local fault slip the shales within the relays will continue to attenuate and will remain unbroken. If the vertical component of the local slip exceeds the thickness of a sand layer, the sand layer will be totally separated on either side of the fault and the shale layers below and above the sand layer will merge together along the fault zone

(Figure 2.4C). If the shale layer is not thick enough, with respect to the fault slip, or depending on its ductility and, perhaps, the rate of fault slip, it is broken at a critical point during the attenuation process and the fault segments within the sand horizons above and below the broken shale link or merge together (Figure 2.4D).

In dip section, the resulting vertical (brittle/ductile) anisotropy is what leads to the segmentation of the normal fault, which in turn is clearly visible on Inline sections of the seismic data from the Niger Delta (Figure 6). A forthcoming Leading Edge paper expatiates on the conceptual model by examining both aerial, downdip and along strike fault segmentation along the Fault X.

MAPPING FAULT SEGMENTS ON SEISMIC

Our first clue to the veracity of the segmentation of normal faults in the subsurface came from a routine inspection of seismic sections from Okan field. Conventional interpretation of Fault X had represented it as a single line from top to bottom on seismic dip sections. We found out on closer inspection of discontinuities in the seismic records that the fault geometry was actually that of separate vertical segments arranged in an en echelon configuration (Figure 2.6). Our cursory survey indicates that the Fault X is made up of at least fourteen dip segments. The sense of stepping is consistently top to the left, that is, the upper segment always steps to the left with respect to an observer standing on the lower segment viewing the upper segment. Interestingly enough, on the seismic section, the fault zone is characterized by variation in segment length, and overlap and width of relay zones from the base to the top. At the upper sections, fault segments are short, overlaps between neighboring segments are short but separation of the neighboring segments are large. In other

words relays are short and narrow. At the lower sections of the fault, the segments become longer and overlaps increase and separations decrease indicating that relays become longer and narrower towards the base where the slip is higher. The amount of overlap ranges from fifty to eighty percent of the segment lengths near the base.

In order to verify the existence and true distribution of the fault segmentation, we carried out very detailed interpretation of the seismic volume available over Okan field. This involved the mapping of tens of seismic horizons and twelve fault segments in greater detail. The mapping was done on an interval of two Dip lines by four Strike lines.

After interpreting the fault segment geometry, we picked up all shale layers in the producing stratigraphic section, using available well log data. For this purpose, Well Y was particularly convenient because of its projectory parallelling the fault in a closer proximity for a greater portion of horizons. The locations and thicknesses of these shale layers were then posted on the seismic sections. Once the segments and the shale layers were displayed on the seismic sections, it was apparent that there is a spatial relationship between segment relays and the locations of the thicker shale units (Figure 2.7). Using the conceptual models presented earlier, we then, interpreted the fault relays as the locations of the shaly fault rock due to smearing of the adjacent thick shale units. To understand the detailed architecture of the fault zones, we decided to investigate the relationship between the fault segments, associated shale units and fault rock architecture by using data from wells whose trajectories passed through the relay zones.

MAPPING SMEARED SHALE WITH WELL LOG DATA

Our conceptual model suggests that shale bodies should be found in the fault relay zones either as a monolithologic unit, or as a mixture of different units. This section explains how we quantitatively mapped smeared shale using wireline logs from wells penetrating the fault under study. Wireline log data from fifteen wells that penetrated across Fault X were used in the analysis (Figure 2.5). The CORRELATION tool of the STRATWORKS application was used to correlate the units across the field. The fault picks in the wells were taken from previous work done by Chevron staff

In deriving the presence of smeared shale in the fault zone penetrated by each well, complete sections in wells close by were correlated and unmatched shale signature was considered extraneous material or smeared shale. Resistivity curves were principally used because of their very constant signature for shale. In addition, gamma ray curves were used to compliment the resistivity. It is assumed that the log signature for the smeared shale will be different from that of shale in normal section either because it is considerably attenuated, or because it is already mixed with other shale units within the fault zone. Figure 2.8 shows an example of smeared shale picked in Well Y.

Results from this analysis indicate that there is a relationship between original shale unit thickness smeared shale thickness and fault throw value. Other workers have considered this relationship in more detail. When expressed as a ratio of the fault throw value to shale unit thickness, we call the Shale Smear Ratio (SSR). For a single shale unit, there is a shale smear developed in the relay zone when the SSR is less than between 4 and 6. When the SSR is greater than between 4 and 6, the smear

developed in the relay zone becomes zero. Such results have been reported from surface mapping activities from the Gulf of Suez (Younes, pers. comm.) and the fluvio-deltaic sequence from England (Lindsay, 1993) as well as subsurface data from other environments (Gibson, 1994).

DETAILED ARCHITECTURE OF RELAY ZONES

In the previous section, we confirmed that the fault segment relay zones do indeed contain smeared shale, from well log data. We also established a relationship between single shale units associated with the fault zones and fault throw values. The next step in the process is to establish the detailed architecture of the relay zones. In order to do this, we set up the following guidelines:

- 1 Define shale units that are continuous across the relay zone, using the relationship of shale thickness to fault throw established for single isolated shale layers above (SSR).
 - 2 Define sand units that are discontinuous across the fault. A sand unit will be discontinuous if its thickness is smaller than the fault throw in that interval.
- Once a sand unit becomes discontinuous across a fault, the shale units smeared along the fault above and below the sand unit merge together as described earlier in the conceptual model.

These considerations were applied to the relay zone where Well Y crossed the fault. Figure 2.9 shows the result of this application and its implication for the detailed architecture of relay zones with the following results:

- a.) Within the outer bounds of Segments 5 and 6 earlier picked on seismic, there exists a third, intermediate segment.
- b.) One of the shale units that pass through the fault zones is discontinuous.
- c.) There is a remnant of a previous segment between the discontinuous shale unit and the neighboring continuous unit.

Figure 2.10 shows the detailed architecture of the relay zones with shale smear over a greater stratigraphic section on Line 158, including a neighboring smaller fault.

SEAL ANALYSIS PROCEDURE

We already mentioned in the introduction, the two permeability-reducing factors responsible for the sealing effect in Niger Delta faults –stratigraphic juxtaposition and shale smearing. For this reason, the analysis of fault seals in the delta follows two principal steps, aimed at characterizing these factors. The first is to construct a reliable juxtaposition diagram across the fault zone. The second step is to characterize the presence of shale smear within the fault zone and its impact on the juxtaposition diagram.

Faults are commonly assumed to be planar discontinuities so that the horizons picked on either side of the discontinuity can be used construct juxtaposition diagrams. From the previous sections of this paper, we have shown that the geometry and architecture of fault zones in the Niger Delta are more complex than hitherto assumed. In addition, we have also shown that the distribution of shale smear can actually be mapped, by using both well log data and seismic data. We discuss in this

section, a procedure for analyzing sealing faults which take into consideration the insight thus gained.

Juxtaposition maps, sometimes called Allan diagrams in reference to Allan (1989), are essentially depth vertical sections along the strike length of a fault, showing the locations on of stratigraphic units on either side of the fault. Several methods have been used for juxtaposition mapping. Bouvier et al (1989) and Jev et al (1993) used fault slicing to evaluate juxtaposition of lithology. Yielding et al (1997) described a juxtaposition plot created from well data. As a first step in our analysis, we created a conventional Allan diagram on Fault X, using the fault slice methodology (Figure 2.12). We took our slices on footwall and hanging wall sections by using fifty traces parallel to the fault trace on either side. Areas that would correspond to sand on sand juxtaposition across the fault are highlighted in Figure 2.13.

In the next step, we made a slice of the seismic volume through the fault relays that had been interpreted on seismic (Figure 2.11b), using the major fault segments. This was designed in order to map the locations of the smeared shale, contained in the relay zones. Figure 2.14 shows the amplitude attribute on the seismic section from this slice. All the parts of the section come from the footwall stratigraphic section, except for the polygons, which are the locations of the segment relays. The orange colors on this section correspond to shale while the black colors correspond to sands. Note that the polygons are largely filled with shale, although areas of sand presence exist.

We combined the relay zone map with the previously made juxtaposition diagram to make one integrated juxtaposition diagram as shown in Figure 2.17. Note the difference between Figure 2.13 and Figure 2.17: The sand-on-sand areas determined from conventional Allan diagram are much less than those in the new juxtaposition diagram in which the smeared shale from the relay zones are included.

PRESSURE BEHAVIOR AND ITS IMPLICATION FOR SEAL INTEGRITY

Differences in hydrocarbon contacts on either side of the fault zone are commonly used in recognizing fault seal. This method is often inadequate with regards to the degree and extent of the fault seal effect. On the other hand, mapping differences in pressure values across the fault zone gives a more comprehensive understanding of fault seal. In this case, we compared the initial bottom hole pressure values on both sides of the fault.

In Okan field, the wells draining reservoirs in the hanging wall block (Figure 2.2) have been producing for several decades. The wells draining reservoirs in the footwall block were drilled much later. We made a plot of the initial bottom-hole pressure values in the Main block against depth. This plot shows a straight-line relationship between the fluid pressure and the reservoir depth, with a gradient value of 0.438, which we assumed to be the 'normal' pressure gradient in the area (Figure 2.15). Next, we added initial bottom-hole pressure data from each of the reservoirs in the Footwall block. A number of the Footwall block reservoirs show substantial deviation from the straight line, meaning that their pressures were already depleted before they were even drilled into. The reservoirs with depleted pressures were thus

determined to be in communication across the fault and are used as a test for the proposed methodology.

SEALING EVALUATION

Figure 2.17 shows areas of sand-on-sand juxtaposition across the fault, with pressure situations indicated, after mapping smeared shale locations onto the fault surface. Hydrocarbon leaks would occur across the fault in such sand-on-sand areas which are not covered by the polygons representing shale smear locations in this figure. Fourteen reservoirs in the Footwall block with complete pressure data were inspected in this manner. Comparing Figure 2.17 to Figure 2.16 gives an indication of the correlation between the mapped shale smear locations and the pressure depletion status of the reservoirs.

The results presented above lend some support for the approach that we have chosen to analyze the sealing capacity of Fault X from the Niger Delta. However, more data would help to confirm its reliability and accuracy.

RESULTS AND DISCUSSIONS

We would now like to discuss our methodology with respect to current methods being used in the analysis of sealing faults. In order to properly characterize a given fault system, its geometry must be well understood. We have shown through our new method utilizing our conceptual model and seismic and well data, how the process of shale smearing leads to a different fault geometry than what is currently

used in seal analysis. This difference has very important implications for the manner in which the rest of the analysis is carried out and final evaluations are made.

As mentioned earlier, an essential first step in the procedure is the construction of juxtaposition maps. In constructing the Allan diagrams conventionally, it is commonly assumed that the fault zone is uniform in thickness and petrophysically transparent such that the lithological units on either side are juxtaposed against each other. This is not strictly correct however, because of the existence of fault rock within the fault zone. The lithologies are actually juxtaposed against the fault rock where it exists, which in this case is mostly smeared shale at relay zones. As such, we may define two types of juxtaposition. The first type is common or conventional juxtaposition, in which the effect of fault rock (smeared shale) is either neglected or statistically distributed along the fault. The second type will be true juxtaposition, in which shale smear and its distribution are taken into account.

Because of the inadequacy of the Allan diagram to fully characterize the fault zone, current methods use the algorithms described earlier to 'fill in' the fault zone with the expected fault rock. Unfortunately, all the algorithms use an averaging technique to distribute certain shaly fault rock over the fault surface. However, we know that the fault rock is distributed in a discrete and systematic manner within the fault zones. The result of this procedural shortcoming is an unrealistic image of the fault architecture, leading to inaccurate prediction of fault seal capacity.

CONCLUSIONS

1. Based on the conceptual model for the development of shale smears, we have interpreted the fault zone into a series of vertically discontinuous segments on seismic. This is in contrast to the common but geomechanically unsound interpretation of fault zones as one vertical continuous 'fault plane'.
2. Along the vertical extent of the fault, we recognize areas of high incidences of localized shale smear, being the relay zones between the fault segments. These areas correspond to stratigraphic horizons of thicker shale layers and are consistent with the conceptual model for the initiation of fault segments at sand/shale boundaries and the development of shale smear at extensional relays. On the other hand, the inter-relay zones are areas of low smear occurrence and possible sand-on-sand contact across the fault. The nature of the fault petrophysical property along these parts is different than those with shale smear and should be evaluated on different grounds.
3. As a result of the foregoing analyses, we determine that most incidences of fault seal occur in reservoirs juxtaposed against relay zones. Most incidences of fault leak occur in reservoirs juxtaposed against the inter-relay zones, where the shale smear is broken up.
4. With this methodology, smear location can be mapped directly and there will be no need to calibrate results in data sets where sealing behavior is documented from well data. However, well data should, of course, be used to test the results.
5. These techniques shall improve our ability to accurately evaluate the capacity of fault seals that have developed as a result of the shale smearing process.

Additional advantages expected to accrue from their use include the possibility of

using commonly available data, equal access to applications for both exploration and production problems.

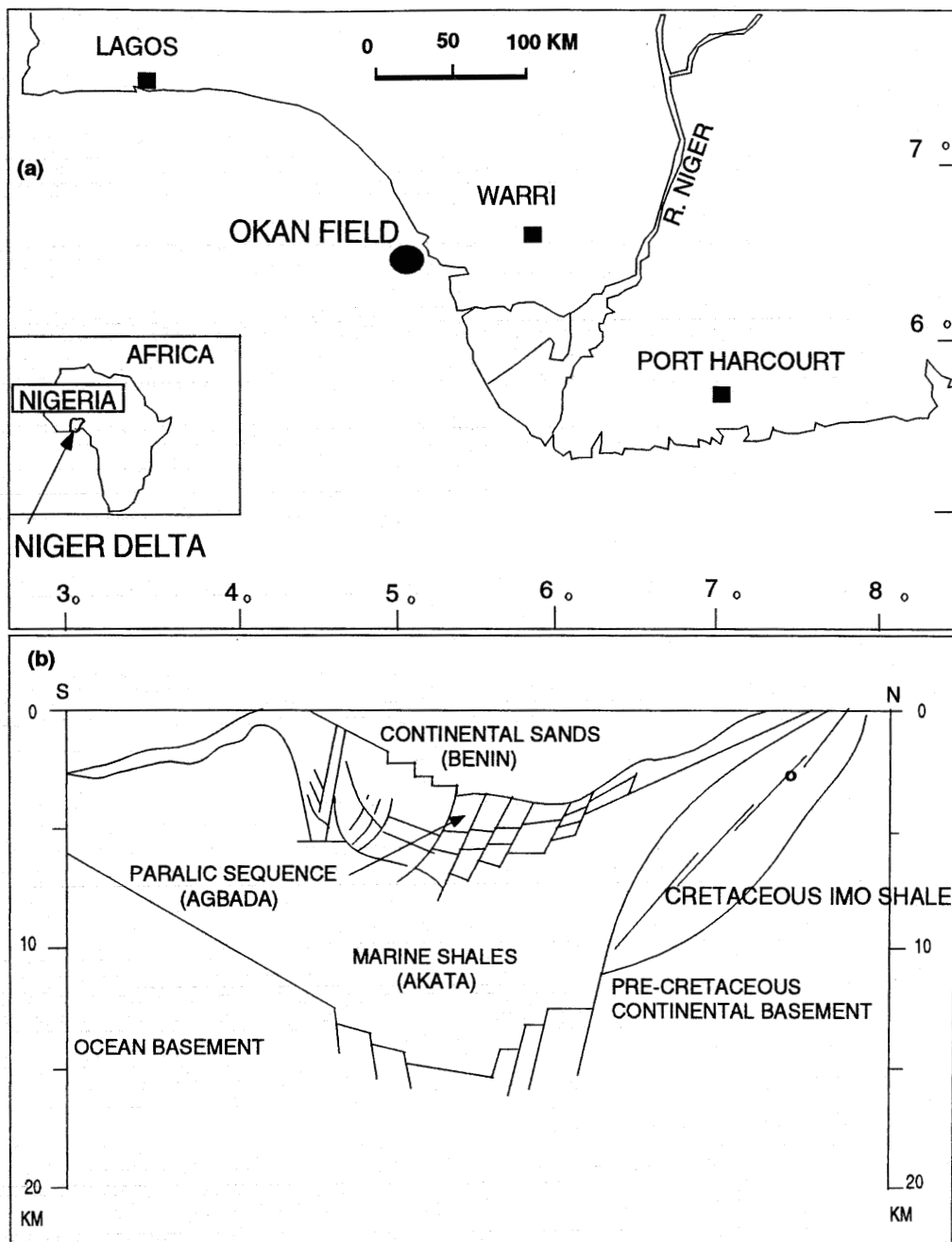


Figure 2.1: (a) Location map of the Okan field and (b) a North-South Crosssection of the Niger Delta, showing tectonic and stratigraphic elements (after Doust and Omatsola, 1989).

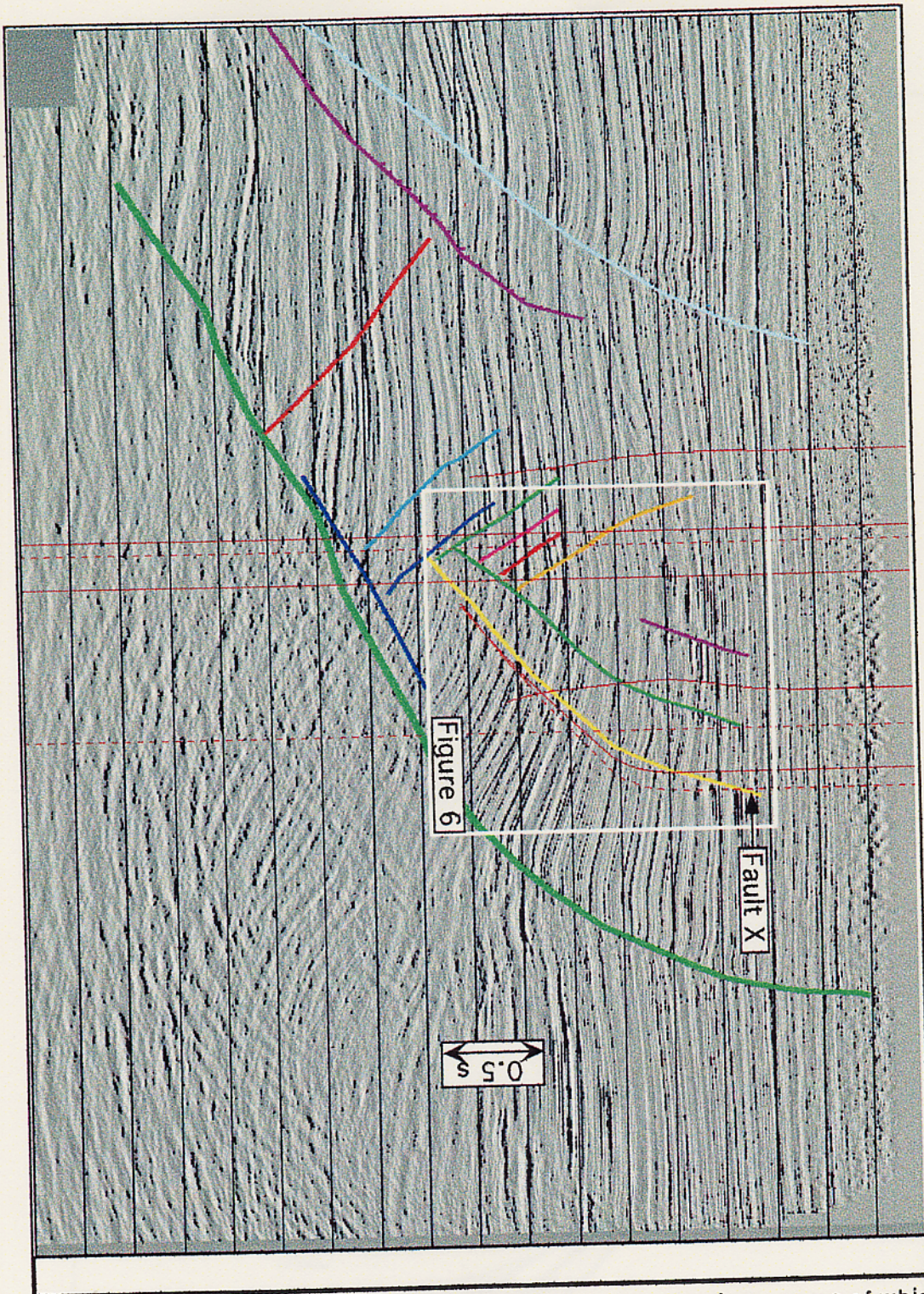


Figure 2.2: Okan megastructure, showing some well projections, some of which cross Fault X.

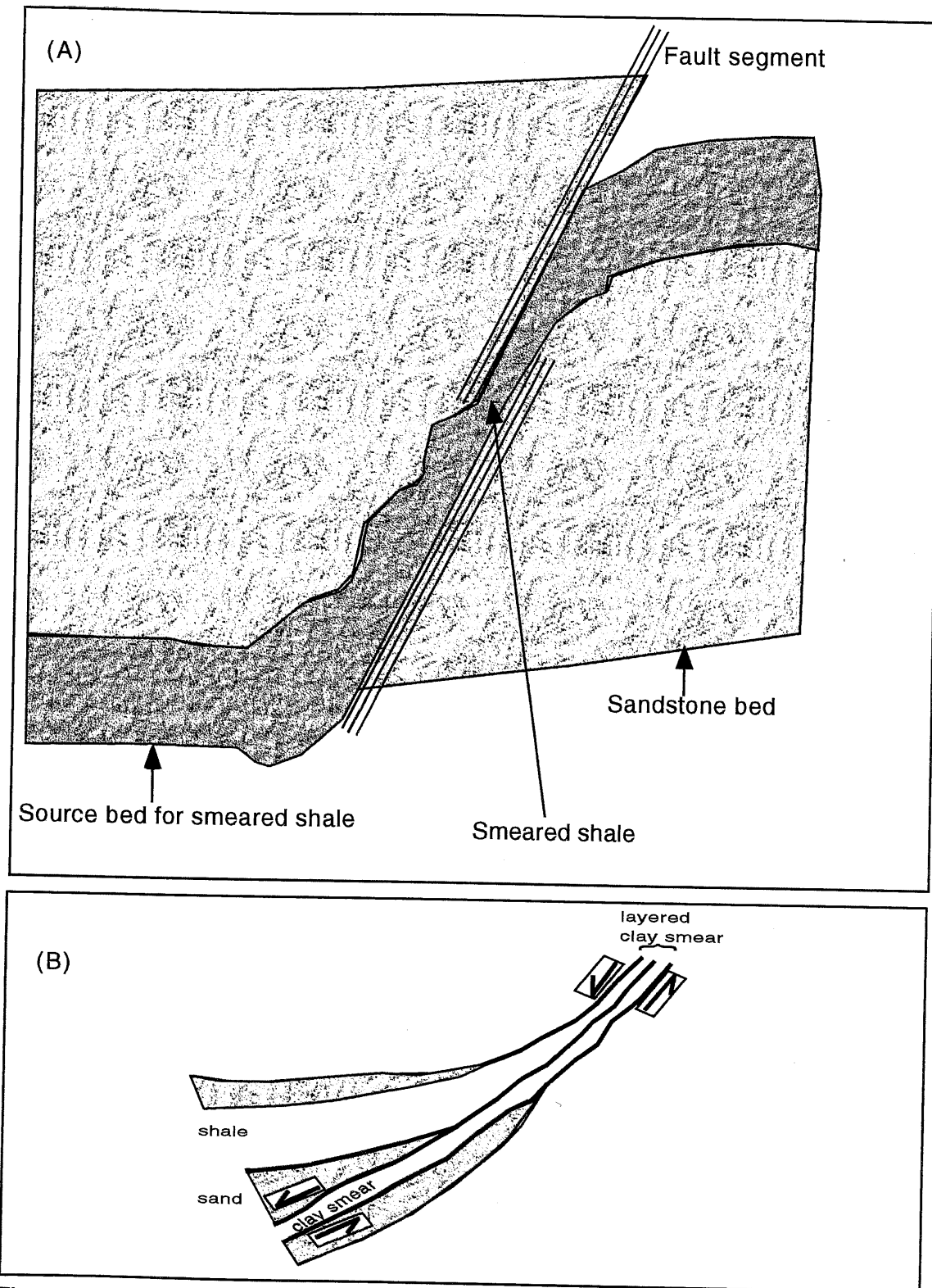
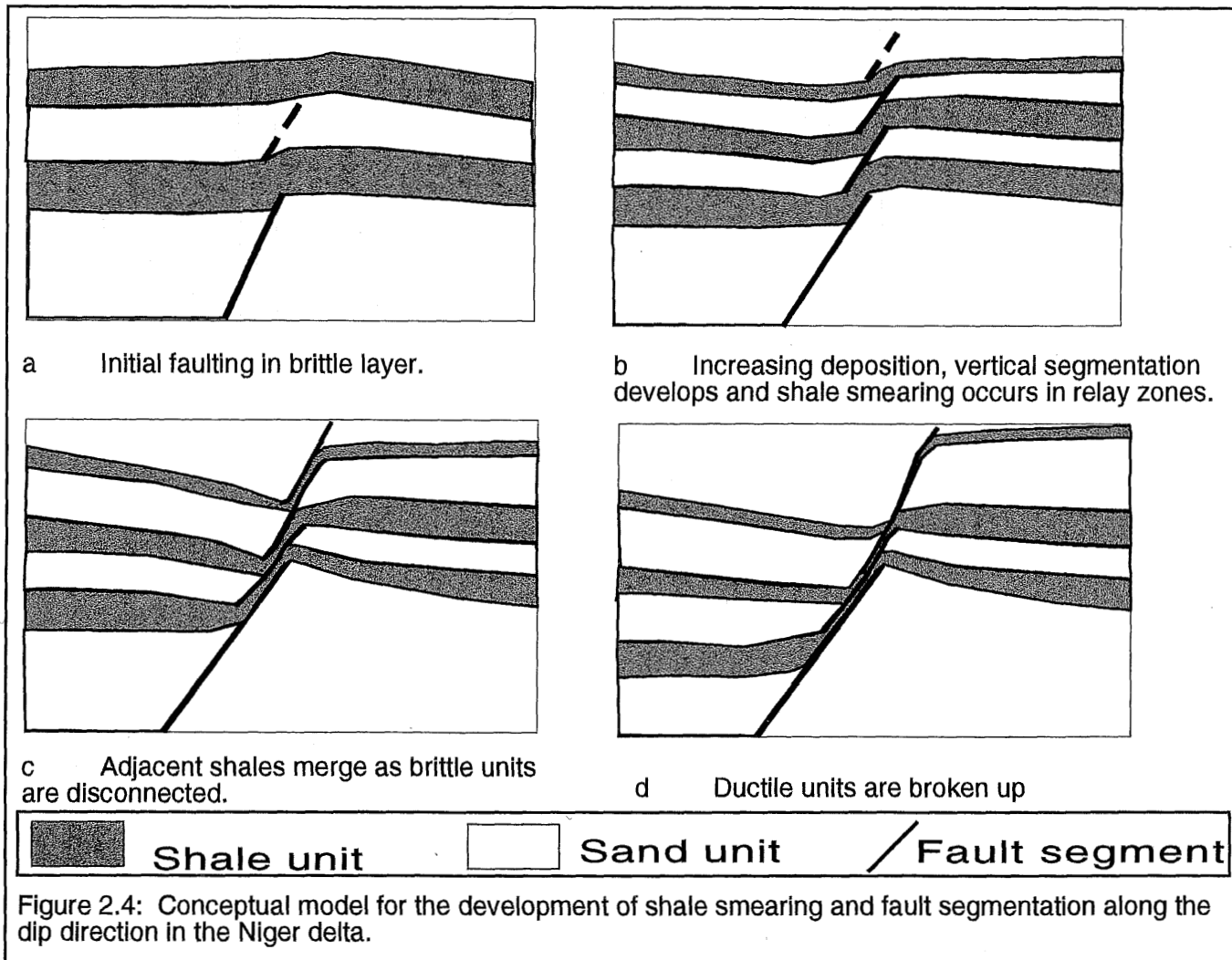


Figure 2.3: (A) Idealized normal fault showing shale smearing and associated structures (modified from Weber et al, 1978); (B) Layered shale smear (modified from Lehner and Pilaar, 1997).



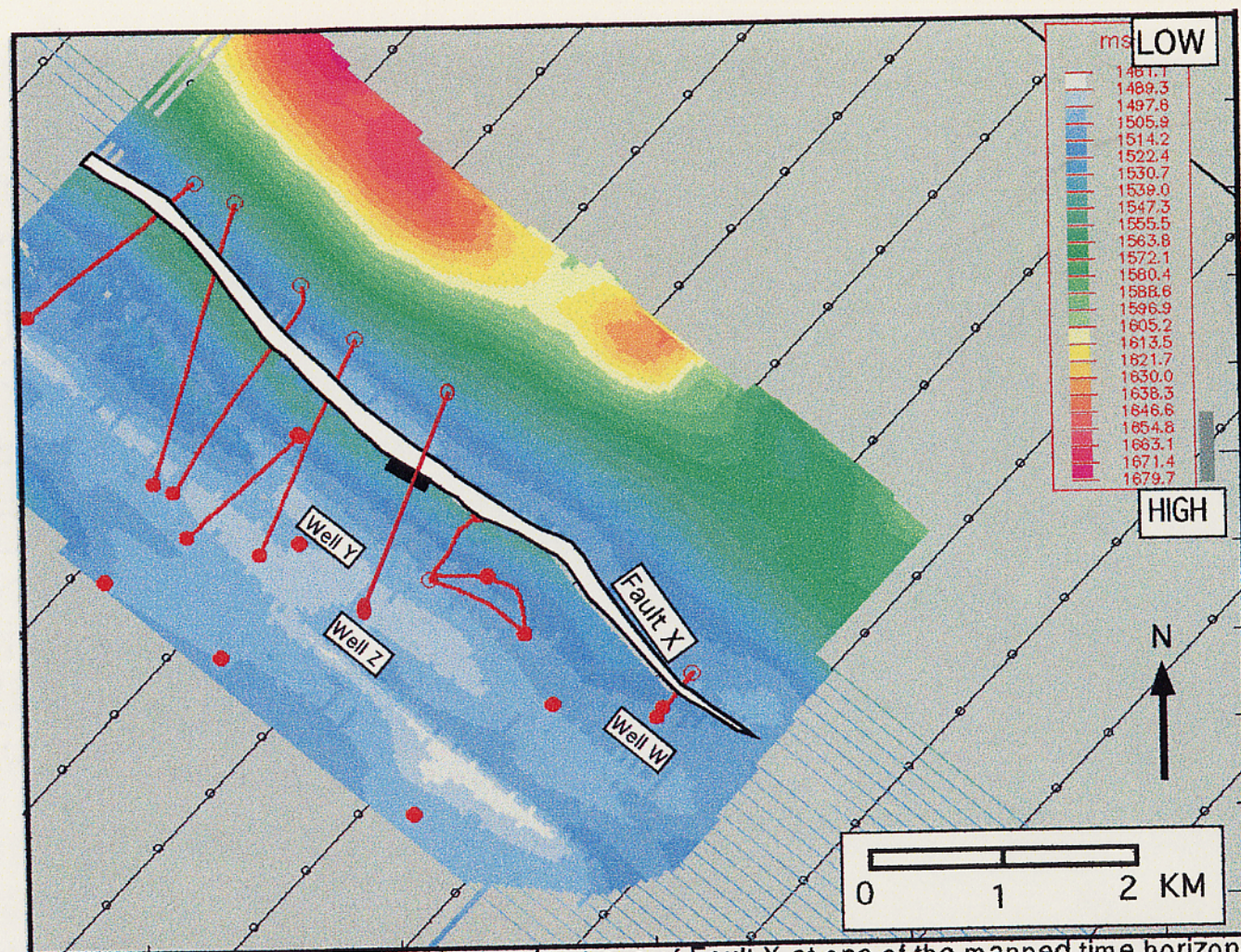


Figure 2.5: Okan field basemap, showing trace of Fault X at one of the mapped time horizons. Structure contour is progressively higher from blue to green to yellow and then to red. The red lines are directional wells while the red points are straight vertical wells. The fault dips to the southwest. Notice many of the wells crossing the fault. Data from Wells Y, Z and W are shown in subsequent figures

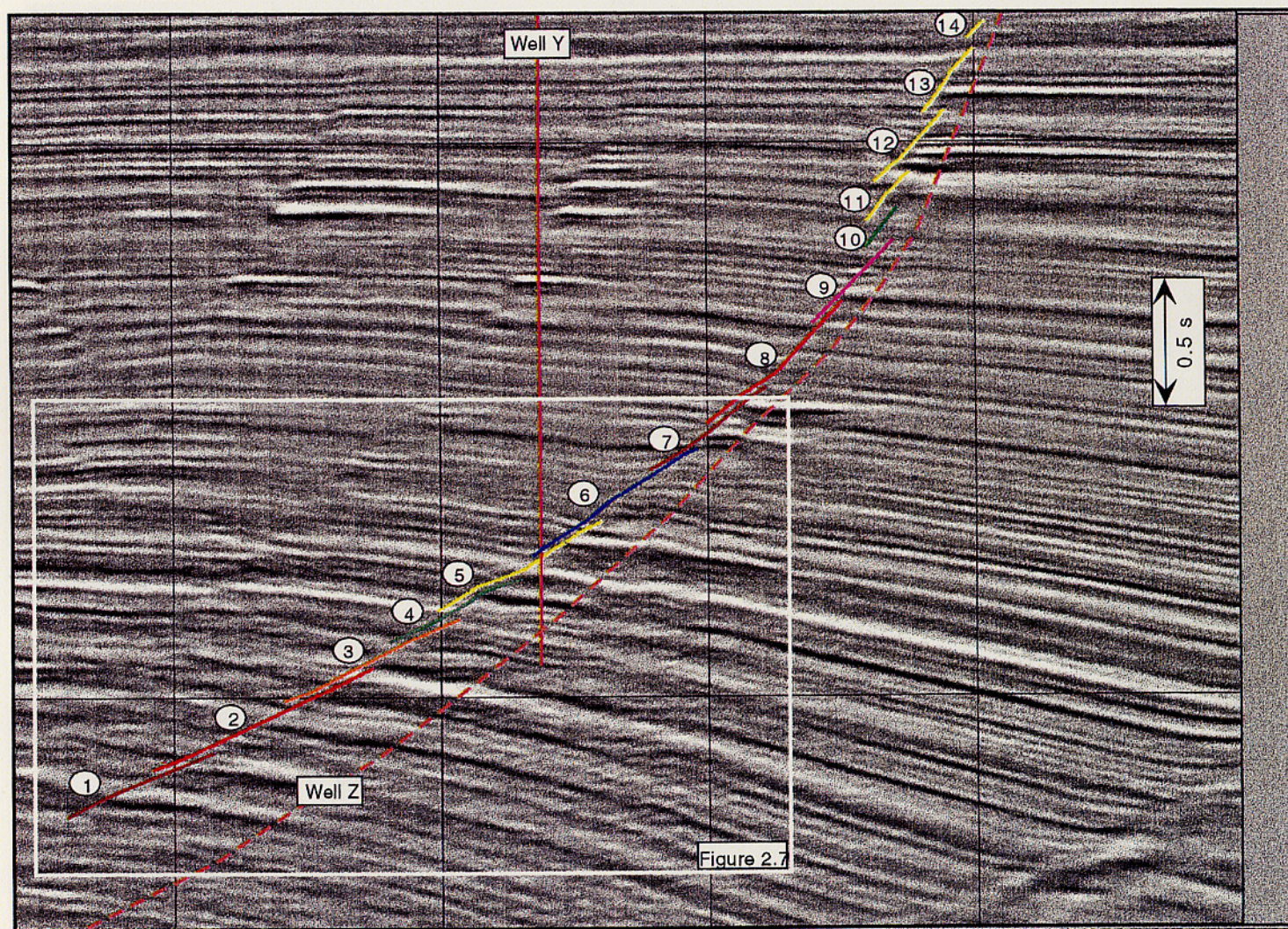


Figure 2.6: Showing major fault segments interpreted on a seismic dip line 1158 and wells providing log data. The segments are numbered from 1 at the base to 14 at the top. The wellpaths for Wells Y and Z are posted. Box shows the location of Figure 2.7.

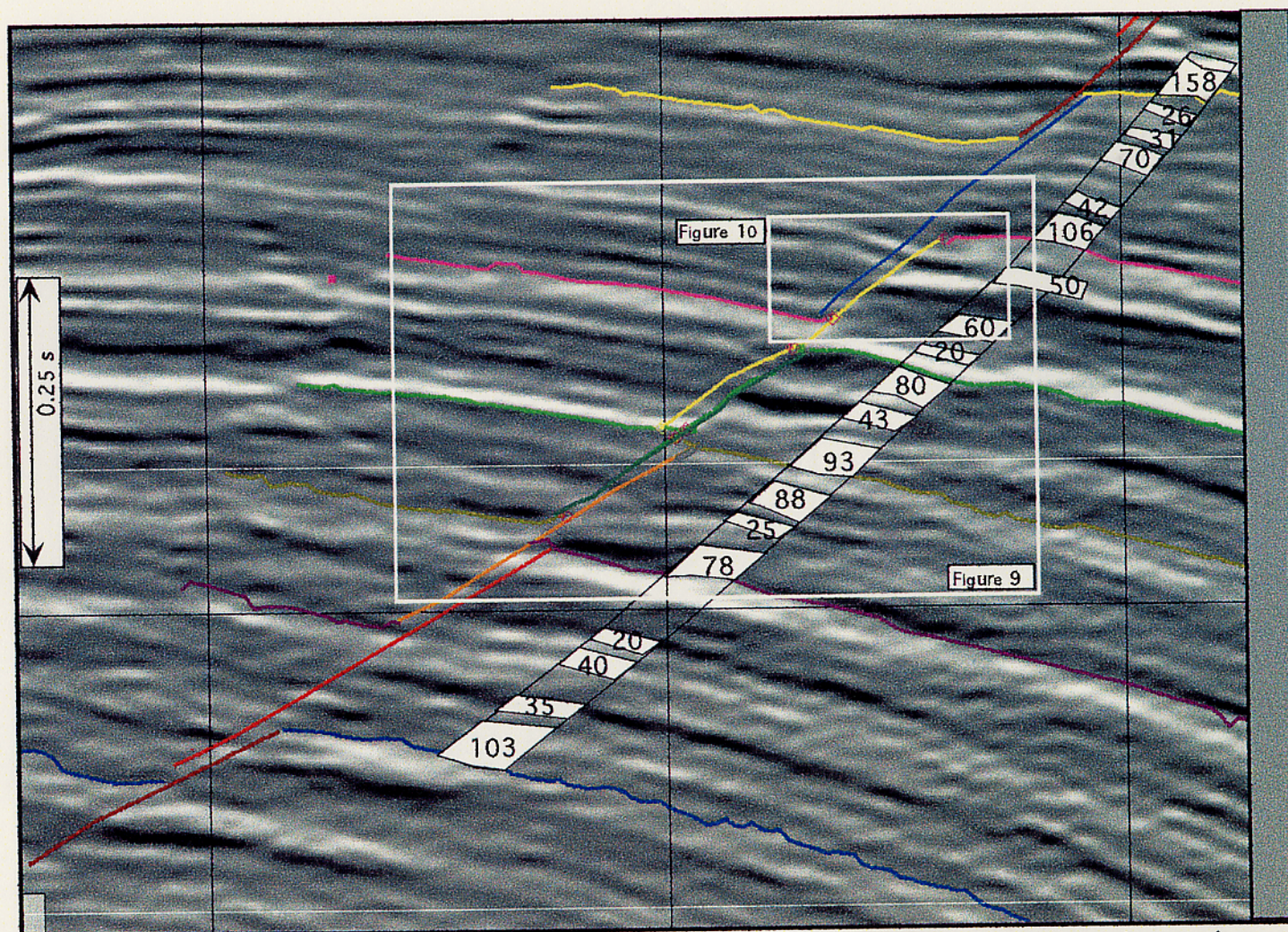


Figure 2.7: A section of seismic dip line shown in Figure 2.6, illustrating the spatial relationship between major fault segment relays and thicker shale units. Only the shale units in the section that are thicker than twenty feet are posted, along the path of Well Z. Colored horizons correspond seismic levels near the thickest shale units.

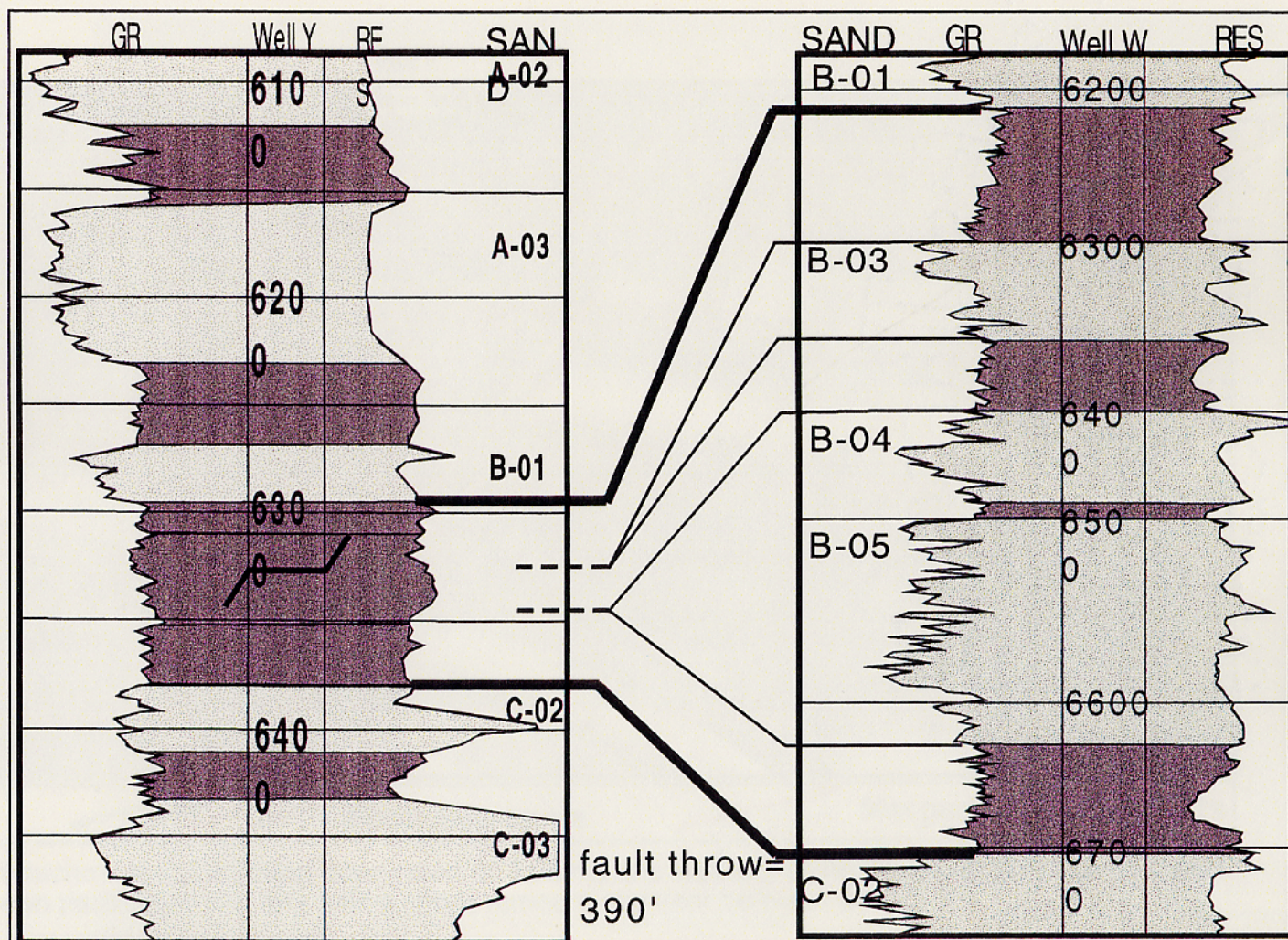


Figure 2.8: Well log correlation section showing smeared shale in Well Y as it crosses Fault X between Segments 5 and 6. GR and RES are Gamma Ray and Resistivity logs, respectively, at a relay. Depth in feet.

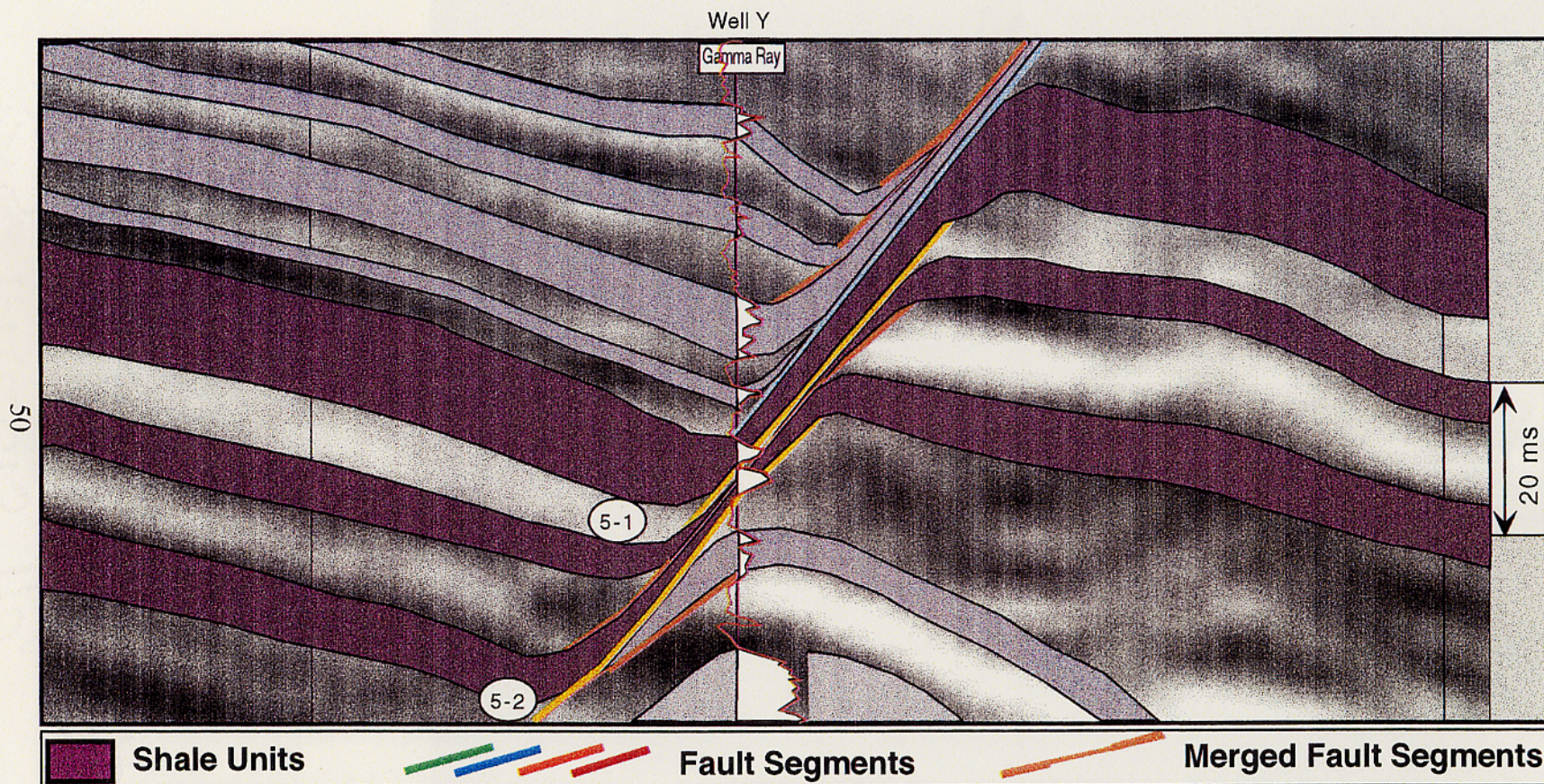


Figure 2.9: Detailed architecture of shale smear interpreted on seismic and well log, using Well Y data. Note how the major Segment 5 has been partitioned into two, with a minor remnant segment between them.

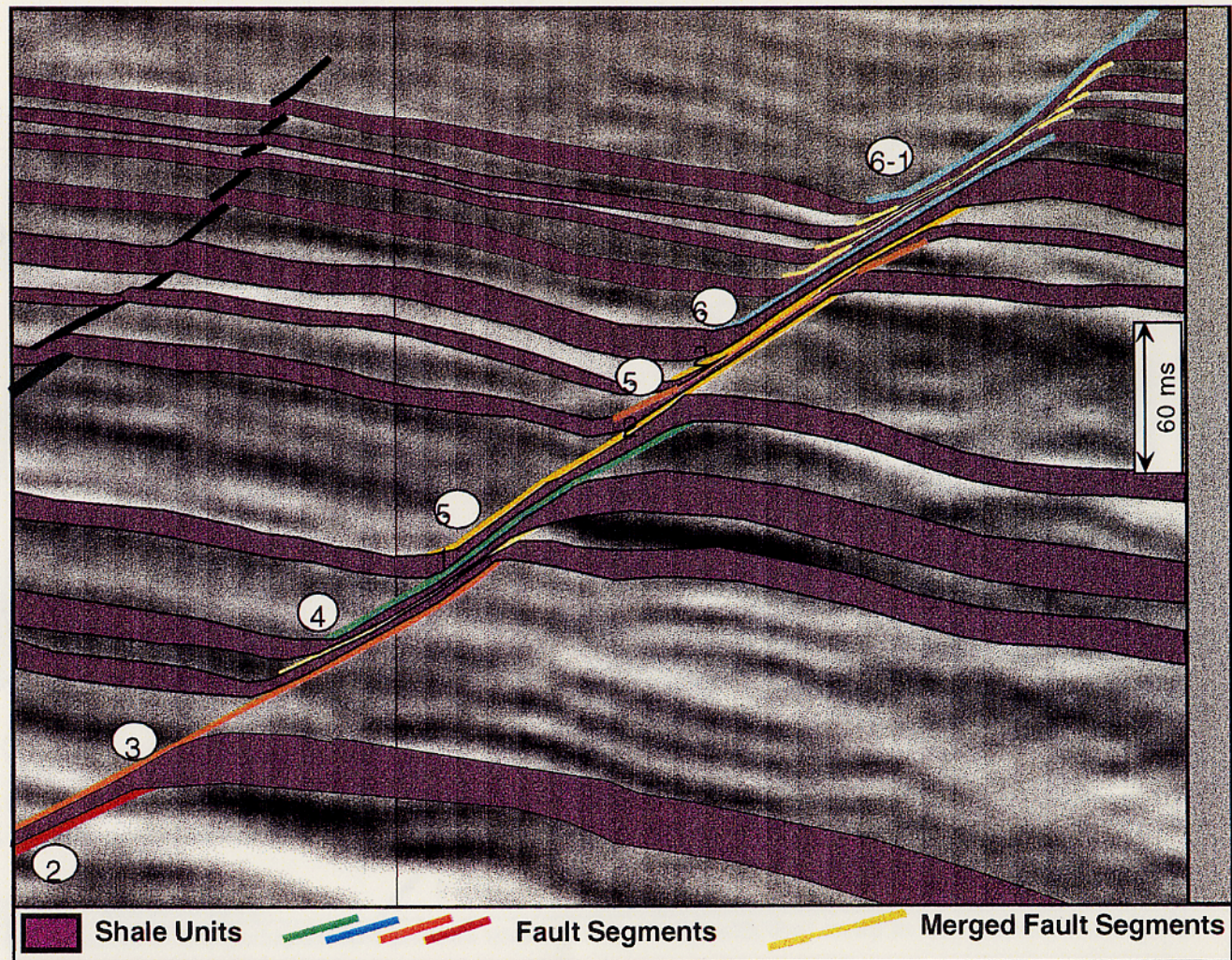


Figure 10: greater section of Dip Line 1158, showing detailed architecture of shale smear interpreted on seismic, with stratigraphic data from nearby wells. Note the complexity of the structure. A neighboring fault with much smaller throw is interpreted for comparison.

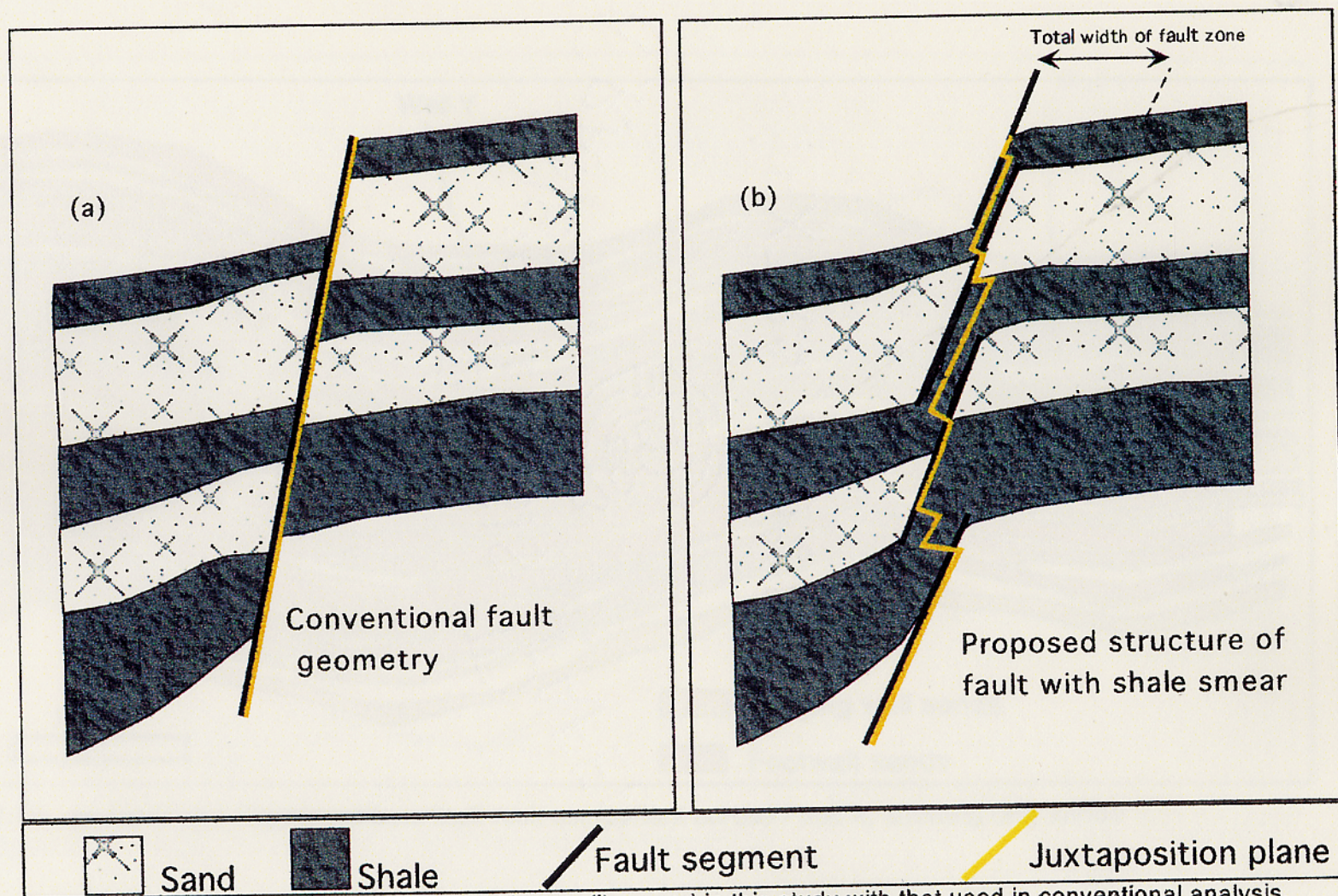


Figure 2.11: A comparison of the juxtaposition profiles used in this study with that used in conventional analysis.

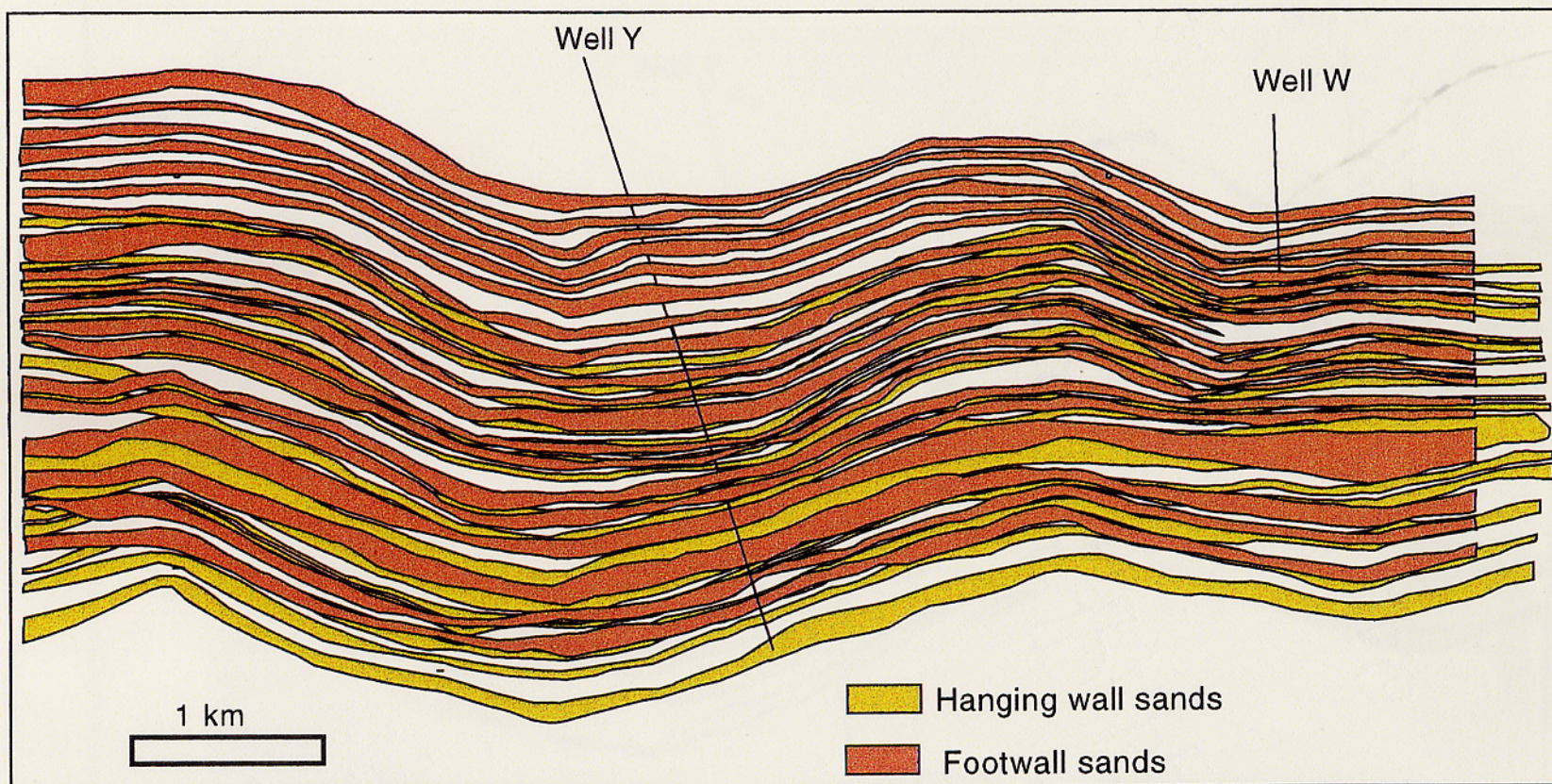


Figure 2.12. Juxtaposition diagram without fault rock component across Fault X, showing only sands.

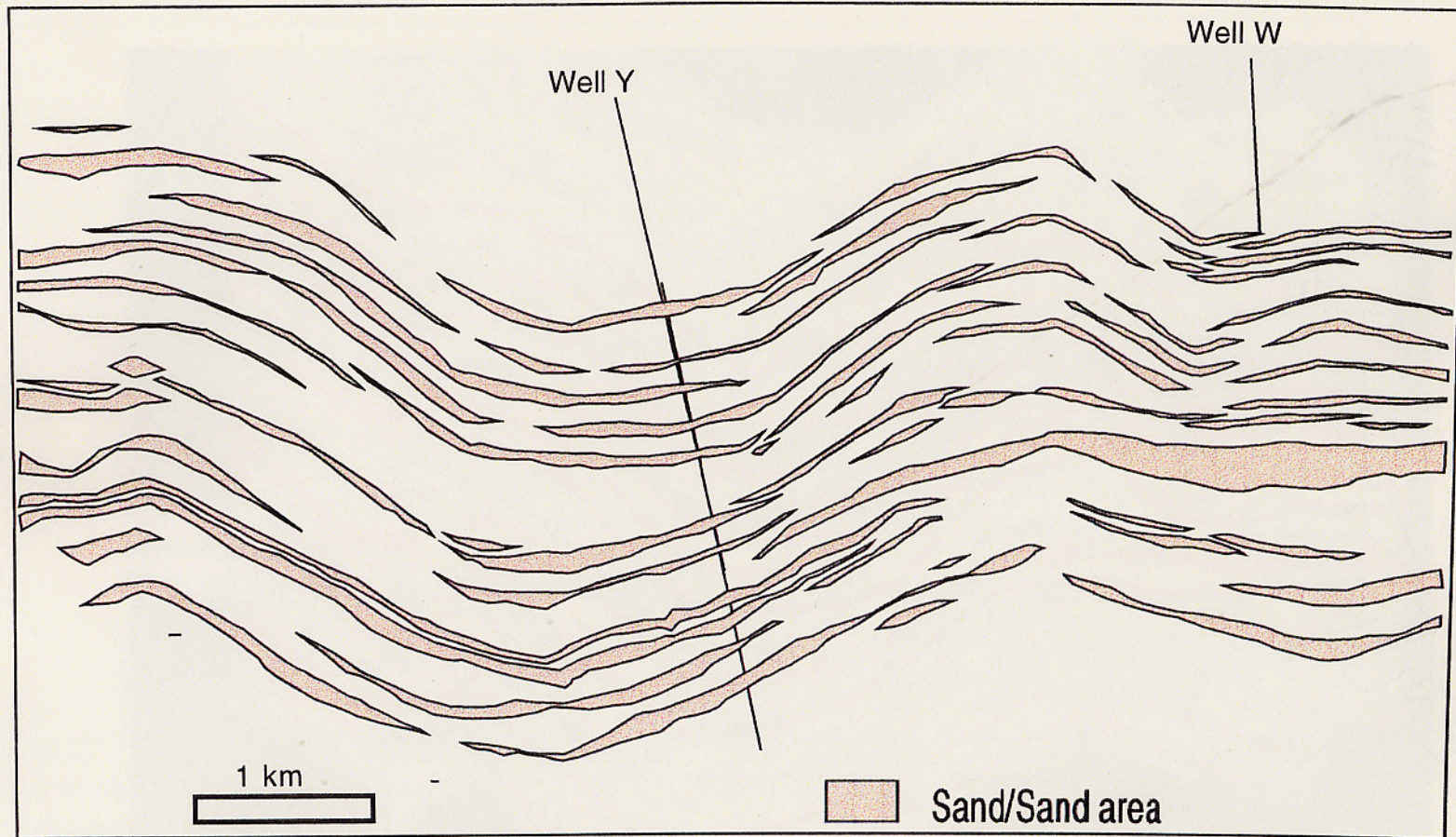


Figure 2.13: Areas of sand/sand contact mapped from Figure 2.12

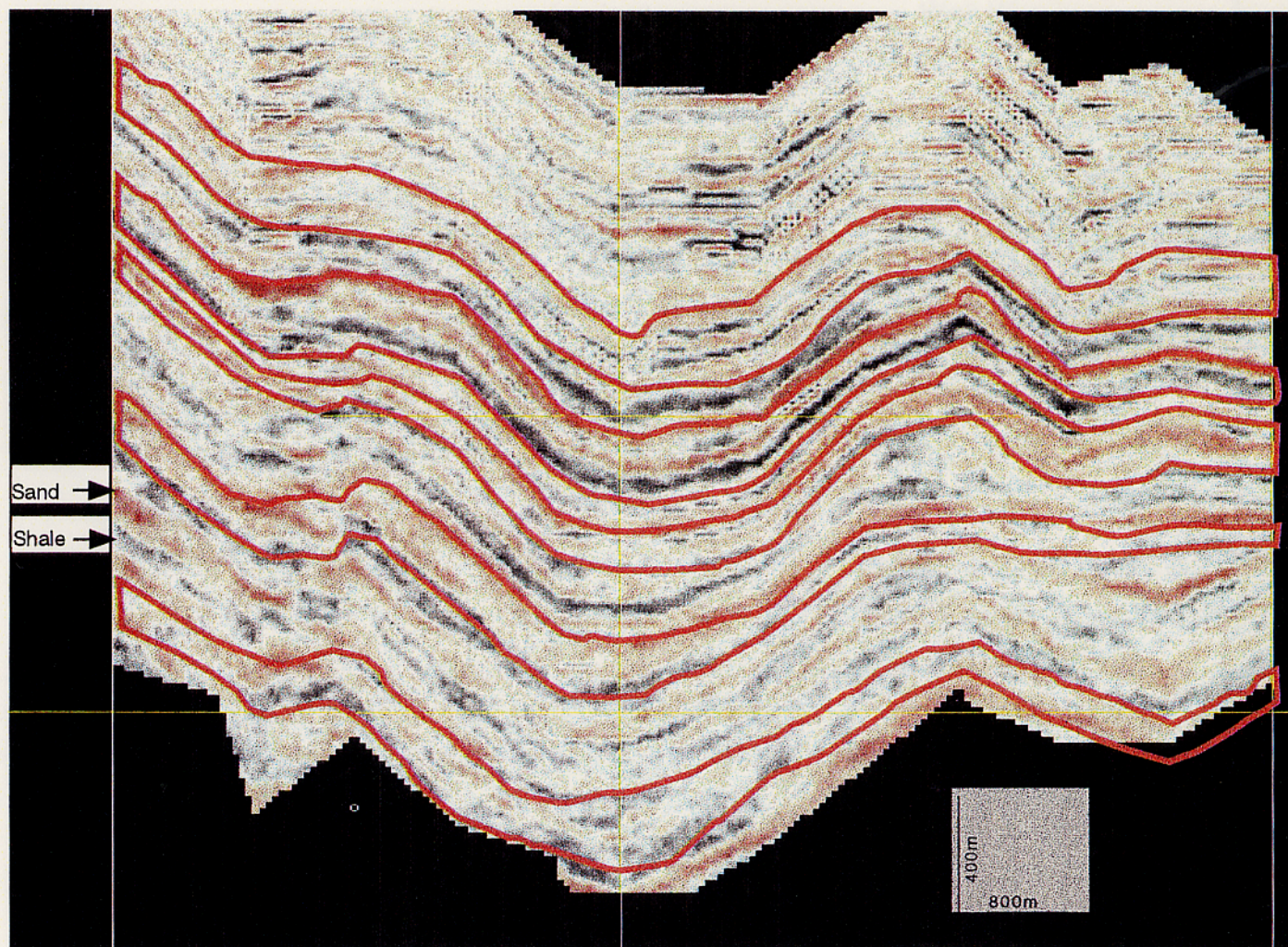


Figure 2.14: Amplitude distribution on the fault surface, using the proposed juxtaposition profile. The orange polygons are the relay zones between major fault segments over the producing interval. Note that the relay zones show concentrations of shale lithology. The yellow lines are seismic line paths.

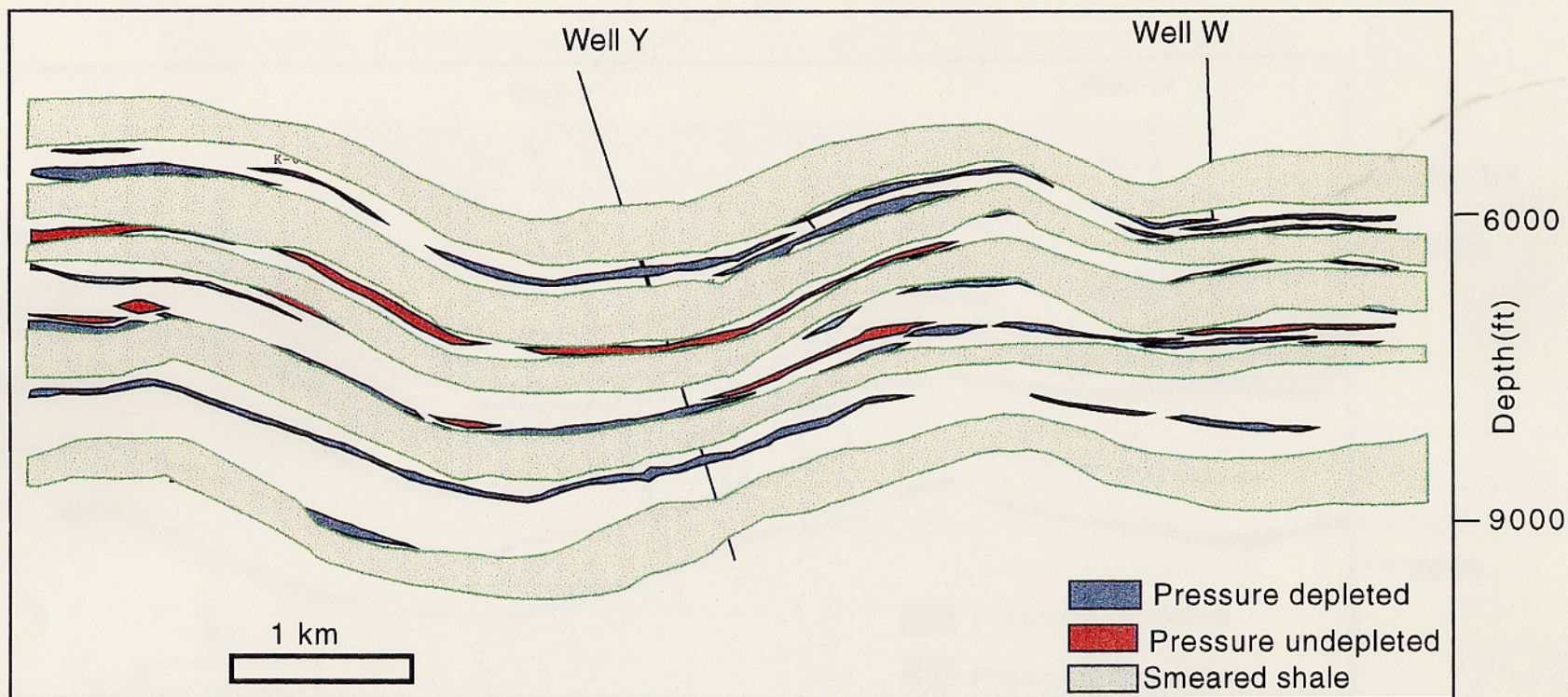


Figure 2.17: Modified juxtaposition diagram incorporating shale smear. The polygons representing smeared shale are the same shown in Figure 2.14. Leaks are expected only where the sand/sand areas are not covered by the shale smear.

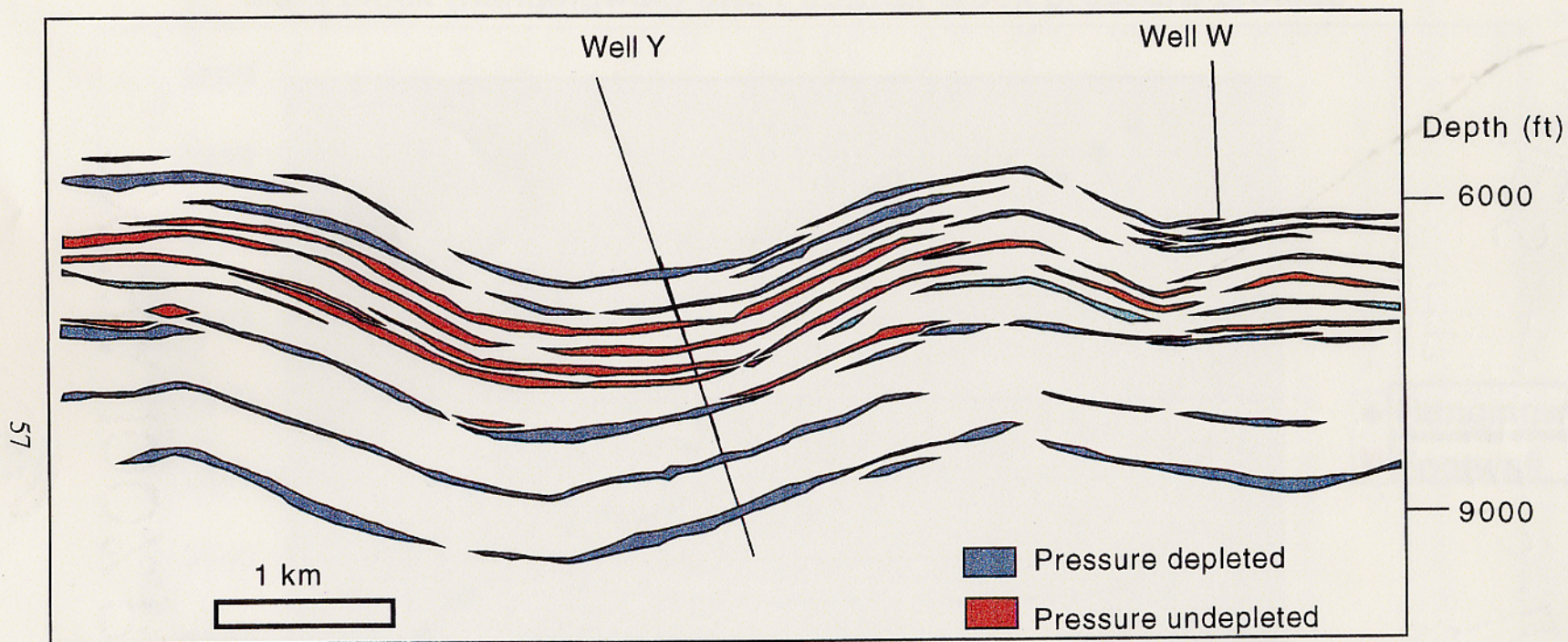


Figure 2.16: Sand/sand areas showing pressure depletion status of the differen reservoirs in the Footwall block.

Main block (hangingwall) and Footwall block pressure profiles

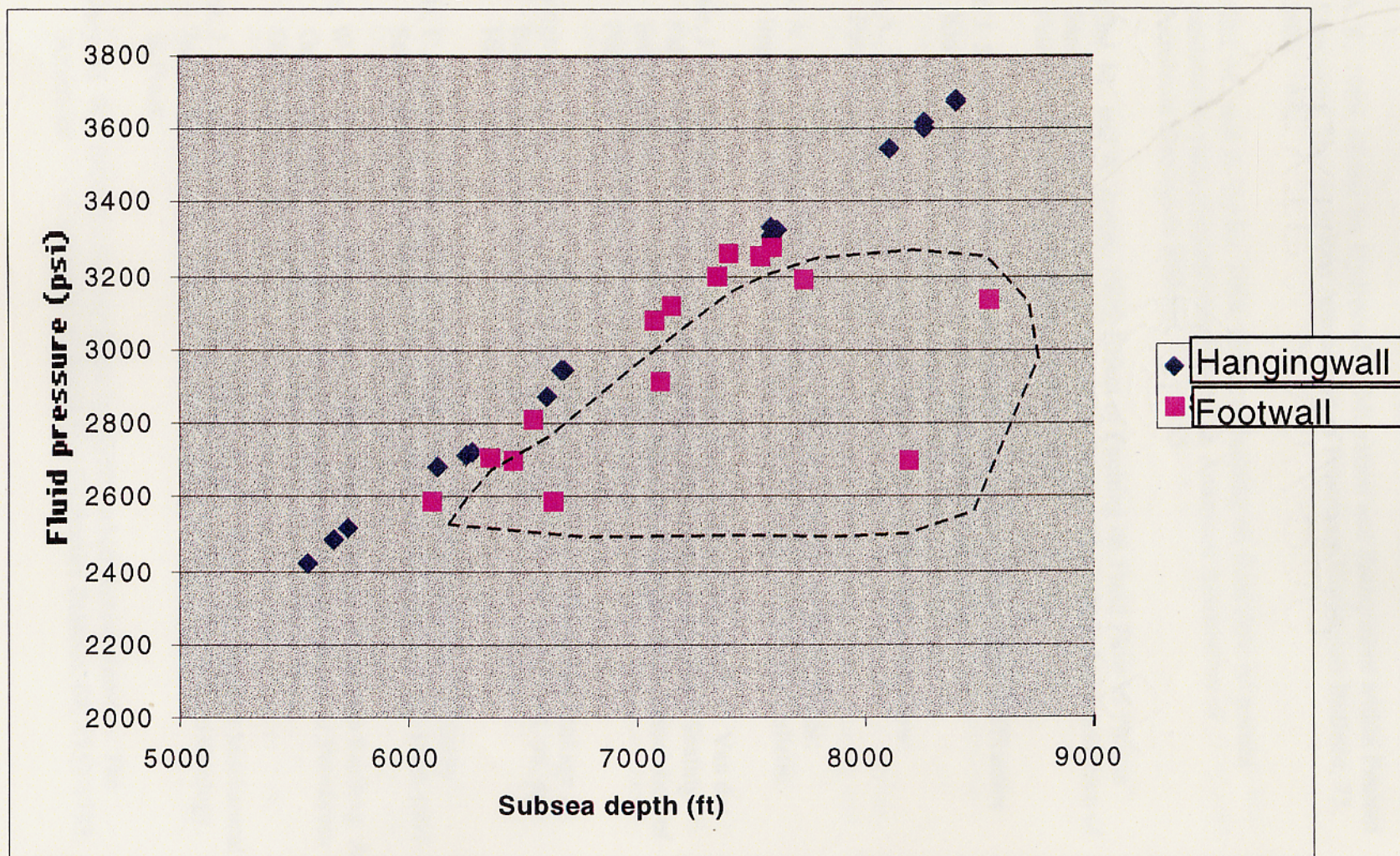


Figure 2.15: Initial bottom-hole pressure profiles for reservoirs in Okan field. The values in the dashed polygon are depleted pressures.

References:

- Allan, A. S., 1989, Model for Hydrocarbon Migration and Entrapment within Faulted Structures: The American Association of Petroleum Geologists Bulletin, 73, 803- 811.
- Antonellini, M., and A. Aydin, 1994, Effect of faulting on fluid flow on porous sandstones: petrophysical properties: The American Association of Petroleum Geologists Bulletin, 78, p. 355-
- Antonellini, M., and A. Aydin, 1995, Effect of Faulting on Fluid Flow in Porous Sandstones: Geometry and Spatial Distribution: The American Association of Petroleum Geologists Bulletin, 79, 642-671.
- Archer, J. S. and Wall, C. G., 1996, Petroleum Engineering Principles and Practice Kluwer Academic Publishers, Dordrecht/Boston, p. 10-11.
- Aydin, A., 1999, Fractures and Faults and Hydrocarbon Migration and Flow: Petroleum Geology (in review).
- Aydin, A. and Y. Eyal, 1999, Anatomy of a Normal Fault with Shale Smear: Implications for Fault Seal Analysis. To be submitted to AAPG Bulletin.
- Bouvier, J. D., K. Sijpesteijn, D. F. Kluesner, C. C. Onyejekwe, and R. C. Van der Pal, 1989, Three-dimensional Seismic Interpretation and Fault Sealing Investigations, Nun river Field, Nigeria: The American Association of Petroleum Geologists Bulletin, 73, 1397-1414.
- Cartwright, J. A. et al, 1996, The Growth of Normal Fault by Segment Linkage In Buchanan, P. G. et al, Geological Society Special Publication, Vol. 99, pp 163- 177.
- Childs, C., Nicol, A., Walsh J. J. and Watterson, J., 1996, Growth of Vertically Segmented Normal Faults, Journal of Structural Geology, vol ,pp 1389-1397.
- Crans, W., G. Mandl and J. Haremboure, 1980, On the Theory Of Growth Faulting: A Geomechanical Delta Model Based On Gravity Sliding: Jouranal of Petroleum Geology, 2, 3, 265-307.
- Crider, J. G. and Pollard, D. D., 1998, Fault Linkage: Three-dimensional Mechanical Interaction Between Echelon Normal Faults, Journal of Structural Geology, In Press.
- Downey, M. W., 1984, Evaluating Seals for Hydrocarbon Accumulations: The American Association of Petroleum Geologists Bulletin, 68, 1752-1763.

- Eisenberg, R. A., R. J. Brenneman, A. A. Adeogba, and U. K. Acharaya, 1996, Integrated fault Seal Analysis, Risk Management and Reservoir Management: Okan Meren Fields, Nigeria: Book of Abstracts-conference on Faulting, Fault Sealing and Fluid Flow in Hydrocarbon Reservoirs, Rock Fracture Deformation Research, University of Leeds.
- Evamy, B. D., J. Haremboure, P. Kamerling, W. A. Knaap, F. A. Molloy, and P. H. Rowlands, 1978, Hydrocarbon Habitat of Tertiary Niger Delta: The American Association of Petroleum Geologists Bulletin, 62, 1-39.
- Gibson, R. G., 1994 Fault-zone Seals in Siliciclastic Strata of the Columbus Basin, Offshore Trinidad: The American Association of Petroleum Geologists Bulletin, 78, 1372-1385.
- Gugliemo, Jr., G., Jackson, M. P. A., Vendeville, B. C., 1997, Three-dimensional Visualization of Salt Walls and Associated Fault Systems, : The American Association of Petroleum Geologists Bulletin, 81, p. 46-61.
- Jev, B. I., C. H. Kaars-Sijpeisteijn, M. P. A. M. Peters, N. L. Watts and J. T. Wilkie, Akaso Field, Nigeria: Use of 3-D Seismic, Fault Slicing, Clay Smearing and RFT Pressure Data on Fault trapping and Dynamic Leakage, : The American Association of Petroleum Geologists Bulletin, 77, 1389-1404.
- Lehner, F. K. and W. F. Pilaar, 1997, On a Mechanism of Clay Smear Emplacement in Synsedimentary Normal Faults, In Norwegian Petroleum Society, eds., Hydrocarbon Seals-Importance for Exploration and Production (conference abstracts) Norwegian Petroleum Society, Oslo. P. 4.
- Lindsay, N. G., F. C. Murphy, J. J. Walsh, and J. Watterson, 1993, Outcrop Studies of Shale Smears on Fault Surfaces, Spec. Publs. Int. Ass. Sediment, 15, 113-123.
- Mansfield, C. S. and Cartwright, J. A., 1996, High Resolution Fault Displacement Mapping From Three-Dimensional Seismic Data: Evidence for Dip Linkage During Fault Growth, Journal of Structural Geology, Vol 18, Nos 2/3, pp 249-263.
- Short, K. C. and Stauble, A. J., 1967, Outline of Geology of Niger Delta: The American Association of Petroleum Geologists Bulletin, 51, 761-779.
- Smith, D. A., 1966, Theoretical consideration of Sealing and Non-sealing Faults: : The American Association of Petroleum Geologists Bulletin, 50, 363-374.
- Smith, D. A., 1980, Sealing and Non-sealing Faults in Louisiana Gulf Coast Salt Basin: The American Association of Petroleum Geologists Bulletin, 64, 145-172.

- Tearpock, D. J. and Bishcke, R. E., 1991, Applied Subsurface Geological Mapping, Englewood Cliffs, N. J., Prentice Hall.
- Walsh, J. J. and Watterson, J., Geometric and Kinematic Coherence and Scale Effects in Normal Fault Systems, From Roberts, A. M., Yielding, G. & Freeman, B. (eds), 1991, The Geometry of Normal Faults, Geological Society Special Publication No 56, P. 193-203.
- Weber, K. J., and E. Daukoru, 1975, Petroleum geology of the Niger Delta: Ninth World Petroleum Congress transactions, 2, 209-221.
- Weber, K. J., G. Mandl, W. F. Pilaar, F. lehner, and R. G. Precious, 1978, the role of Faults in Hydrocarbon Migration and Trapping in Nigerian Growth Structures, In Tenth Annual Offshore Conference Proceedings, 4, 2643-2653.
- Weber, K. J., 1987, Hydrocarbon Distribution Patterns In Nigerian Growth Fault Structures Controlled By Structural Style and Stratigraphy: Journal of Petroleum Science and Engineering, 1, 91-104.
- Willemse, E. J. M., 1996, 3D Mechanics and Evolution of Discontinuous Faults, Stanford University, Ph. D. thesis.
- Yielding, G., B. Freeman and T. Needham, 1996, In-situ Calibration of Algorithms for Fault-seal Prediction: Book of Abstracts- Conference on Faulting, Fault Sealing and Fluid Flow in Hydrocarbon Reservoirs, Rock Fracture Deformation Research, University of Leeds.
- Yielding, G., Freeman, B. and Needham, D. T., 1997, Quantitative fault seal prediction, The American Association of Petroleum Geologists Bulletin, 81, No. 6, P. 897- 917.

Appendix A- Shale Smear Analysis Using Well Logs

Introduction

This appendix describes the methodology for the interpretation and quantification of shale smear in fault zones using well log data. The analysis helped to develop the conceptual model discussed in Chapter 1.

Several workers have carried out studies to characterize shale smearing. General conclusions from the studies include the following: (1) thicker source beds produce thicker shale smears, (2) shear-type smears decrease in thickness with distance from the source layer, (3) multiple source beds can result in a composite shale smear (Yielding et al, 1997); (4) relative smearing potential increases with the number of source beds passing a point on the fault.

The studies mentioned above have used data either directly collected from the field (Younes and Aydin, 1997; Lehner and Pilaar, 1996; Aydin and Eyal, 1995; Lindsay et al, 1993, Weber et al, 1978) or remotely collected from the subsurface (Yielding et al, 1997; Gibson, R. G., 1994; Bouvier et al, 1989). While field circumstances permit the highest resolution and details necessary, they mostly do not provide reservoir-scale structures. Particular problems are: finding faults with composite shale units that are involved in the smearing process and, or, finding fault throws that are comparable to reservoir scale faults. On the other hand, the main problems with the use of subsurface data include the scarcity of such data, due to both the cost and the difficulty of obtaining them, as in cores and borehole images; as well as the relatively limited resolution that the available data, like wireline logs and pressure data, can provide for shale smear mapping. These reasons might explain why no attempt has been made before now to measure the thickness of smeared shale in fault zones using subsurface data.

Algorithms for shale smear quantification

The factors mentioned above have been used to develop a number of algorithms that seek to quantify the smear values at particular points along the fault zone. Yielding et al (1997) provide an excellent discussion on the different algorithms currently used for shale smear analysis. A central hypothesis of the aforementioned studies is that shale is a ductile material which can flow and stretch during faulting, smearing the surface of the faults (Younes and Aydin, 1997; Lehner and Pilaar, 1996; Aydin and Eyal, 1995; Weber et al, 1978). Younes and Aydin have defined a parameter called the Shale Smear Ratio, which, like others, relates the shale source thickness, the smeared shale thickness and the fault throw. It basically defines a limiting ratio of fault throw to shale source thickness that will cause a total breakdown of the deformed shale in the downdip direction along the fault zone, making the smear thickness equal to zero (Figure A.1). When the SSR is less than a range between 4 and 6, there is a shale smear developed in the fault zone. When the SSR is greater than a range between 4 and 6, the thickness of the shale smeared in the fault zone becomes zero. (Modified from Younes and Aydin, 1997).

$$\text{Shale Smear Ratio (SSR)} = \frac{\text{Fault offset}}{\text{Original shale thickness}}$$

Methodology

Following is the methodology adopted to achieve the foregoing objectives:

1. Use stratigraphic and structural correlation tools to identify and measure smeared shale thicknesses and fault offset values in wells penetrating fault zones
2. Isolate cases in which single shale units are involved in the smearing process and compare the structural, geometric and stratigraphic relationships with that from previous work

3. Define sand units that are continuous or discontinuous across the fault. Sand units that are thicker than the fault throw will continue across the fault (Figure A.2c).
4. Define shale units that are continuous, using the relationship of shale thickness to fault throw established for single isolated shale layers from surface studies to determine cutoffs.
5. Recognize cases in which only single shale units are continuous across the fault and then compare with data from the field.
6. Where multiple shale units are continuous across the fault, measure the total thickness of the shale units forming the smear and calculate a composite shale unit by using the additive value of the unit thicknesses.
7. Test to see if there is any relationship between composite shale thickness, smear quantity and fault throw by making a plot of the smear thickness against fault throw values.

Mapping smeared shale thickness

Wireline log data from fifteen wells that penetrated across the fault under study were used in the analysis. The CORRELATION tool of the STRATWORKS application was used to correlate the units across the field. The fault picks in the wells were taken from previous work done by Chevron staff

In deriving the thickness of shale smeared in the fault zone penetrated by the well, complete sections in wells close by were correlated and unmatched shale signature was considered extraneous material or smeared shale. Resistivity curves were principally used because of their very constant signature for shale. In addition, gamma ray curves were used to compliment the resistivity. It is assumed that the log signature for the smeared shale will be different from that of shale in normal section either because it is considerably attenuated, or because it is already mixed with other shale units within the fault zone (Figure A.2a, A.2b, A.2c). Other parameters

measured included the vertical separation, thicknesses of the missing sand and shale units, bed dips and fault dips. The measured smear thicknesses were later corrected for fault dip to arrive at true smear thicknesses (Figure A.3).

In determining that a single shale layer is involved in the smearing process, the correlation tool shows that only one shale unit is missing or reduced from the normal section as seen in nearby wells. On the other hand, multiple shale units are missing in the particular well with the fault cut when multiple shale units are involved. In either case, if the unit(s) are discontinuous in the fault zone, then only a juxtaposition of units above and below them in the normal section is seen, that is, smear measured will be zero. If the unit(s) are only thinned to a fraction of their original thickness, then some value of the smear will be measured.

Determining fault throw and slip

Fault throw was determined using the equation:

$$\text{Vertical Separation} = \text{ABS} [(\text{Tan of bed dip} / \text{Tan of fault dip}) - 1] / \text{Throw}$$

The bed and fault dips are taken clockwise from 0 to 180 degrees. (Tearpock and Bischke, 1991).

The missing section measured in the wells was equated to the vertical separation. The dip of each bed was determined from the depth map of the bed in question. The dip of the fault at each well location was similarly determined from a fault surface map. The dip slip on each occasion was then determined from the value of the throw (Figure A.4).

Results and discussion

Table A.1 shows the measured parameters from the 15 well-points, including the calculated fault throw and slip. Figure A.5 shows the structural configuration defining the various parameters presented.

From the results shown in Table A.1, the following conclusions may be made:

1. We have been able to measure thicknesses of shale smeared into fault zones penetrated by wells in the Niger delta.

2. Only two single, isolated layers of shale and their corresponding smear thicknesses were measured, due to the large scale of faulting, as is typically encountered in producing fields. Obviously, we can not use this sparse data content to determine the relationship between shale source thickness, smear and fault throw. However, the Shale Smear Ratios calculated from these points fall within the limiting ratios documented from previous study (Younes and Aydin, 1997; Lindsay et al, 1993) (Table A.2, Figure A.2a).

3. When the individual shale source units are discriminated based on their Shale Smear Ratios, and single continuous units are selected and used in the analysis, the results show a decrease in shale smear thicknesses with fault throw, both of which have been normalized by the shale source thicknesses. (Figure A.2b, A.5). This result increases our confidence in the analysis.

4. When the remaining multiple shale units were added together and their thicknesses (normalized by the additive original shale layer thickness) were plotted against the fault throw (normalized similarly), the gradual and systematic nature of the relationship appears to disappear (Figure A.2b, A.6). This trend seems to indicate that the effect of multiple original shale layers is not simply additive when a composite shale smear is formed. For example, it is plausible that the thickness of smeared shale may increase during faulting if several sand layers become discontinuous and several shale layers collapse into a mature fault zone over a small throw window. It may also be simply because the individual shale layers being stretched undergo different thinning fractions at the particular location of the well cut.

Conclusions

Shale smearing in the Niger delta shows a decrease with increasing fault throw when a single shale source is involved in the smearing process. This result is in agreement with behavior documented from other parts of the world. However, for

smearing developed from multiple shale source units, smeared shale thicknesses appear not to show any regular trend with increase in fault throw. More work needs to be done in order to understand exactly how composite shale layers contribute to smear thicknesses in the fault zone during the process of smearing. Important results of this study include our ability, demonstrated here, to measure thicknesses of shale smear from common wireline data and a proposed procedure on how to interpret these data for the specific process and quantity of smearing with respect to original stratigraphy.



IS
14

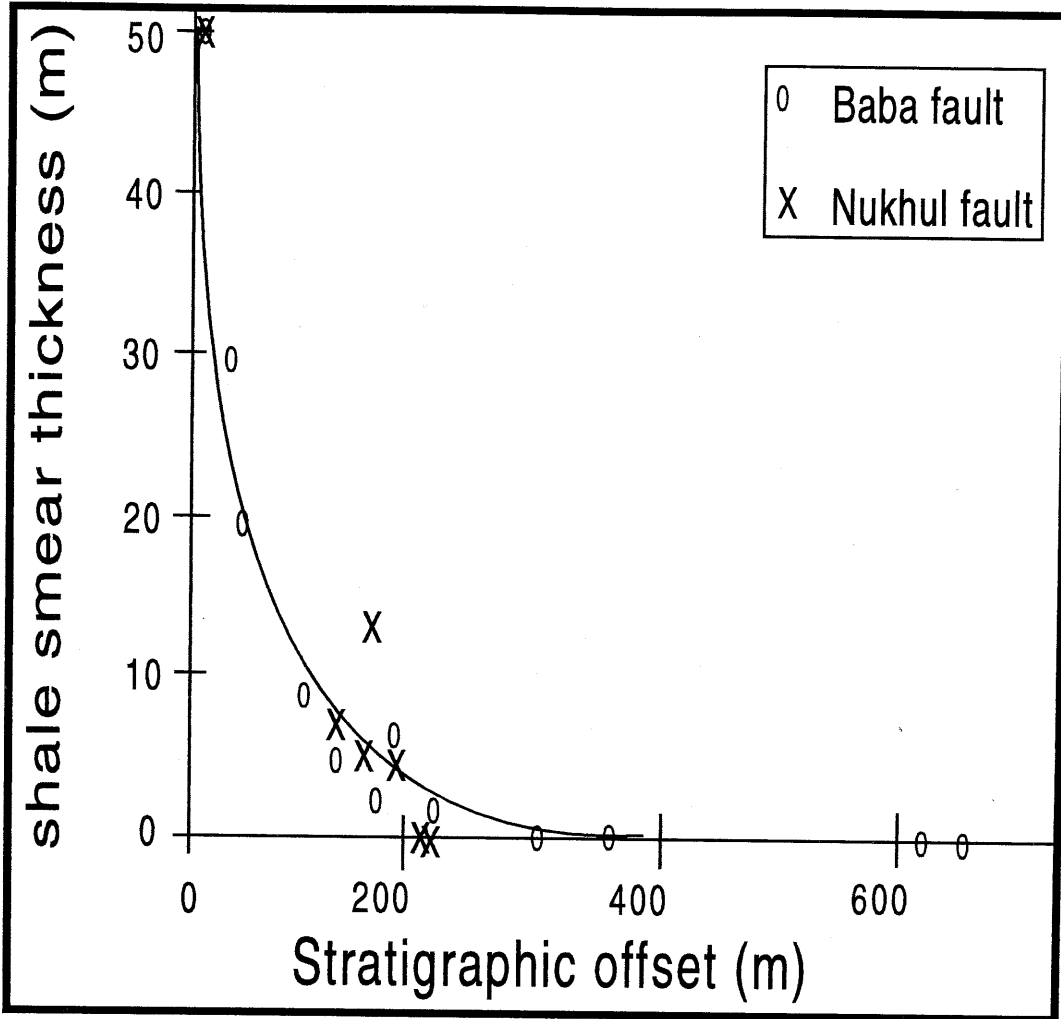


Figure A.1: Relationship between original shale thickness, smeared shale thickness and fault offset. When the SSR is less than a range of 4-6, there is a shale smear developed in the fault zone. When the SSR is greater than a range between 4-6, the thickness of the shale smeared into the fault zone becomes zero. (Modified from Younes and Aydin, 1997).

$$\text{Shale smear ratio (SSR)} = \frac{\text{fault offset}}{\text{original shale thickness}}$$

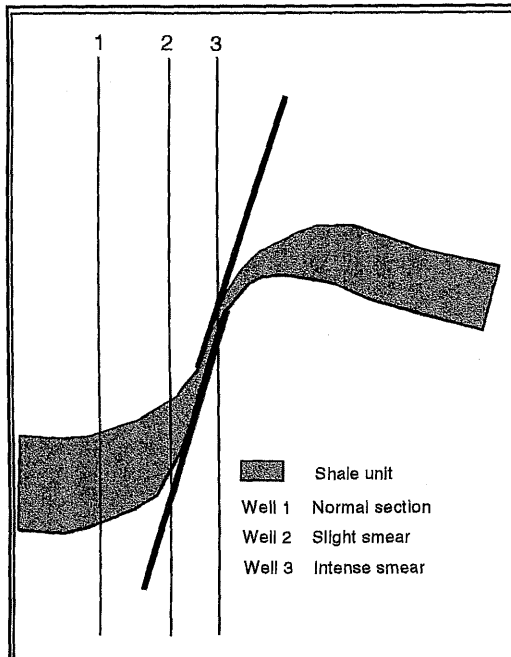


Figure A.2a: Range of smear intensity recorded in different wells: single shale source.

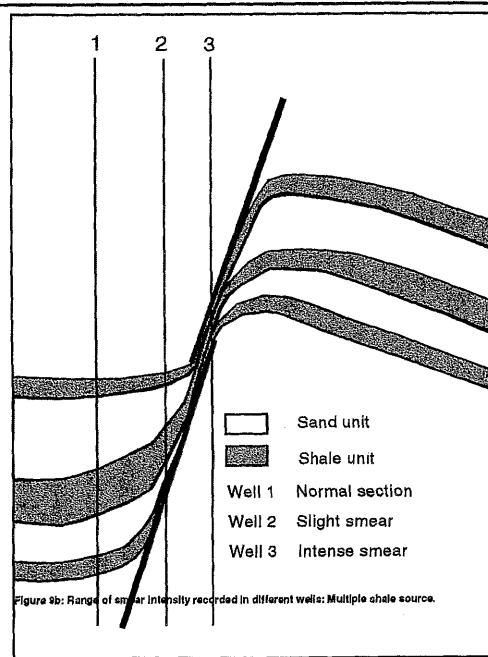


Figure A.2b: Range of smear intensity recorded in different wells: single shale source.

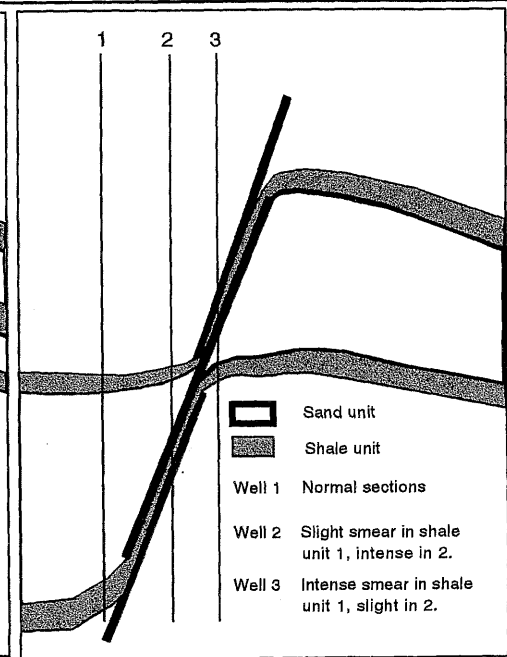


Figure A.2c: Range of smear intensity recorded in different wells: Multiple shale source when sand thickness is greater than fault throw.

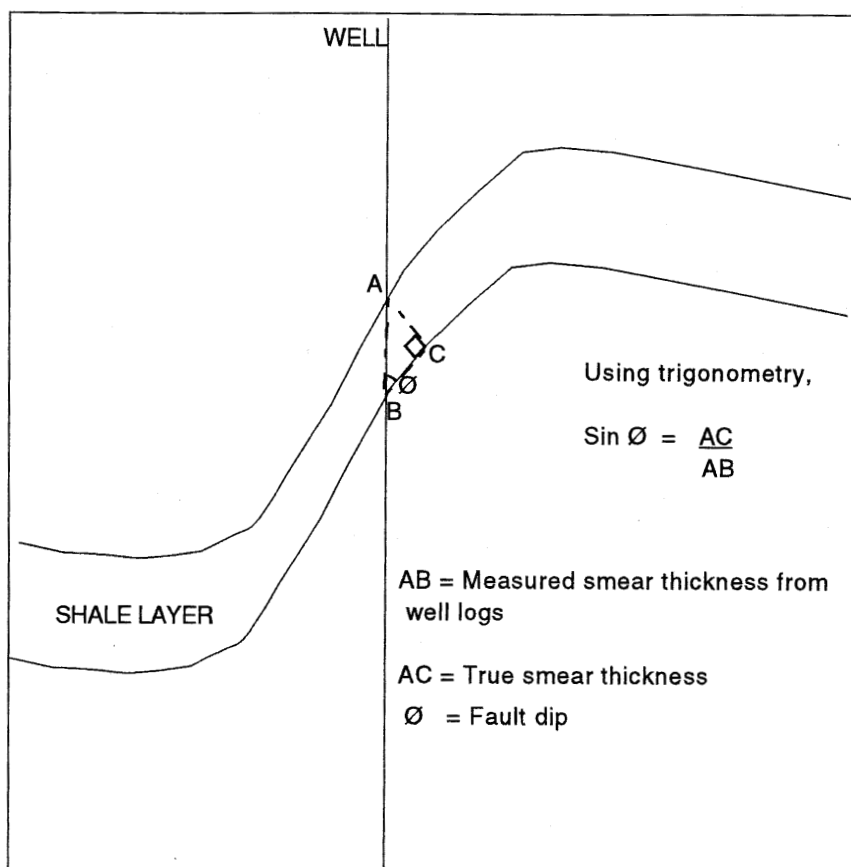


Figure A.3: Showing measured smeared shale thickness and correction for fault dip.

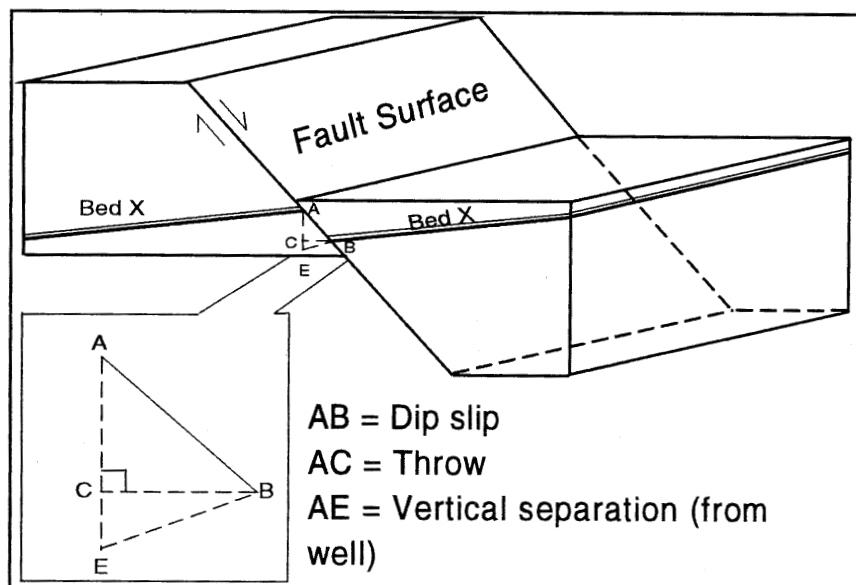


Figure A.4: Block diagram of Bed X displaced by normal fault, illustrating the different fault components in Table A.1 (Modified from Tearpock and Bishcke, 1991)

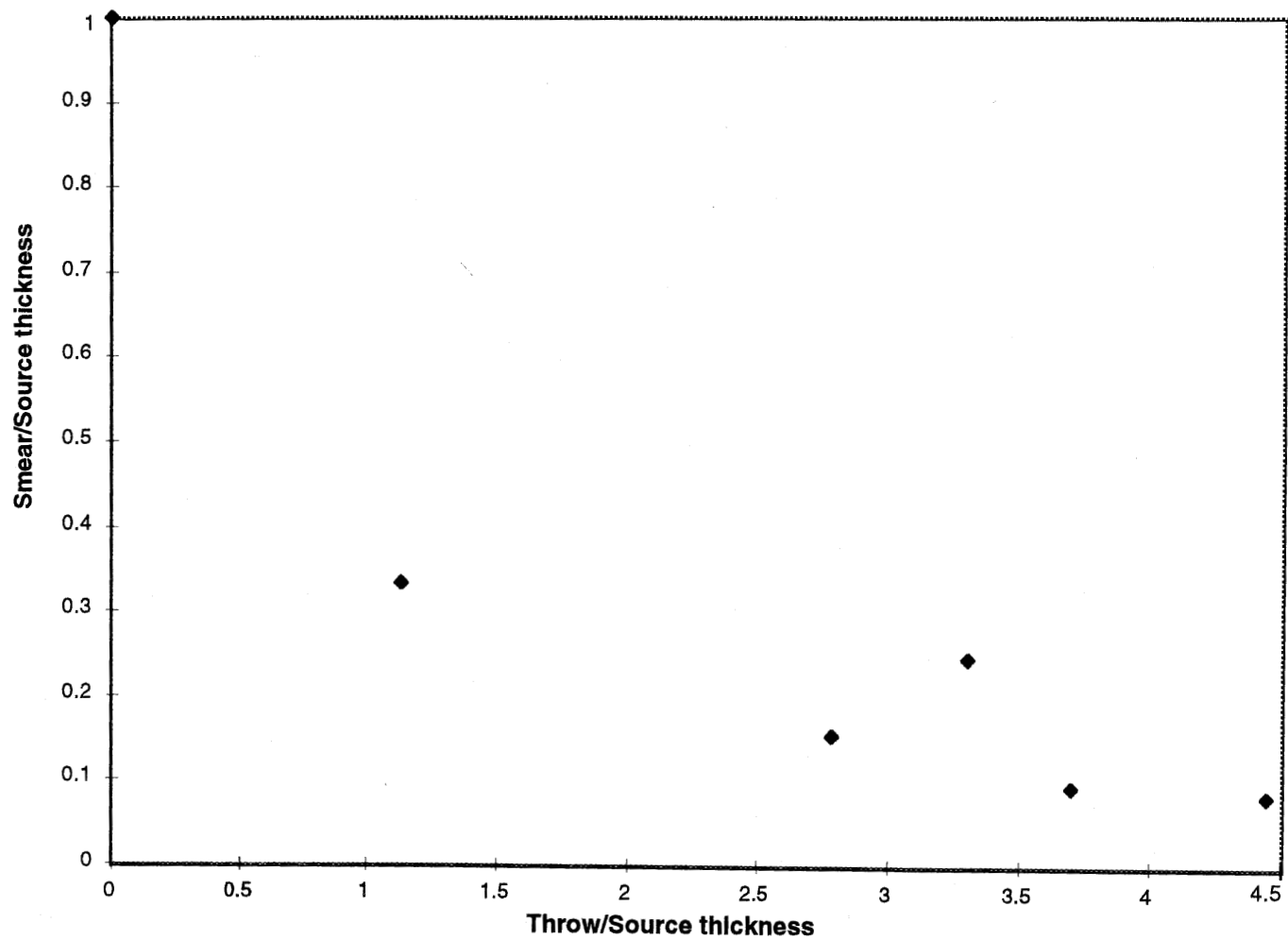


Figure A.5: Normalized shale smear (single unit) vs. normalized fault throw.

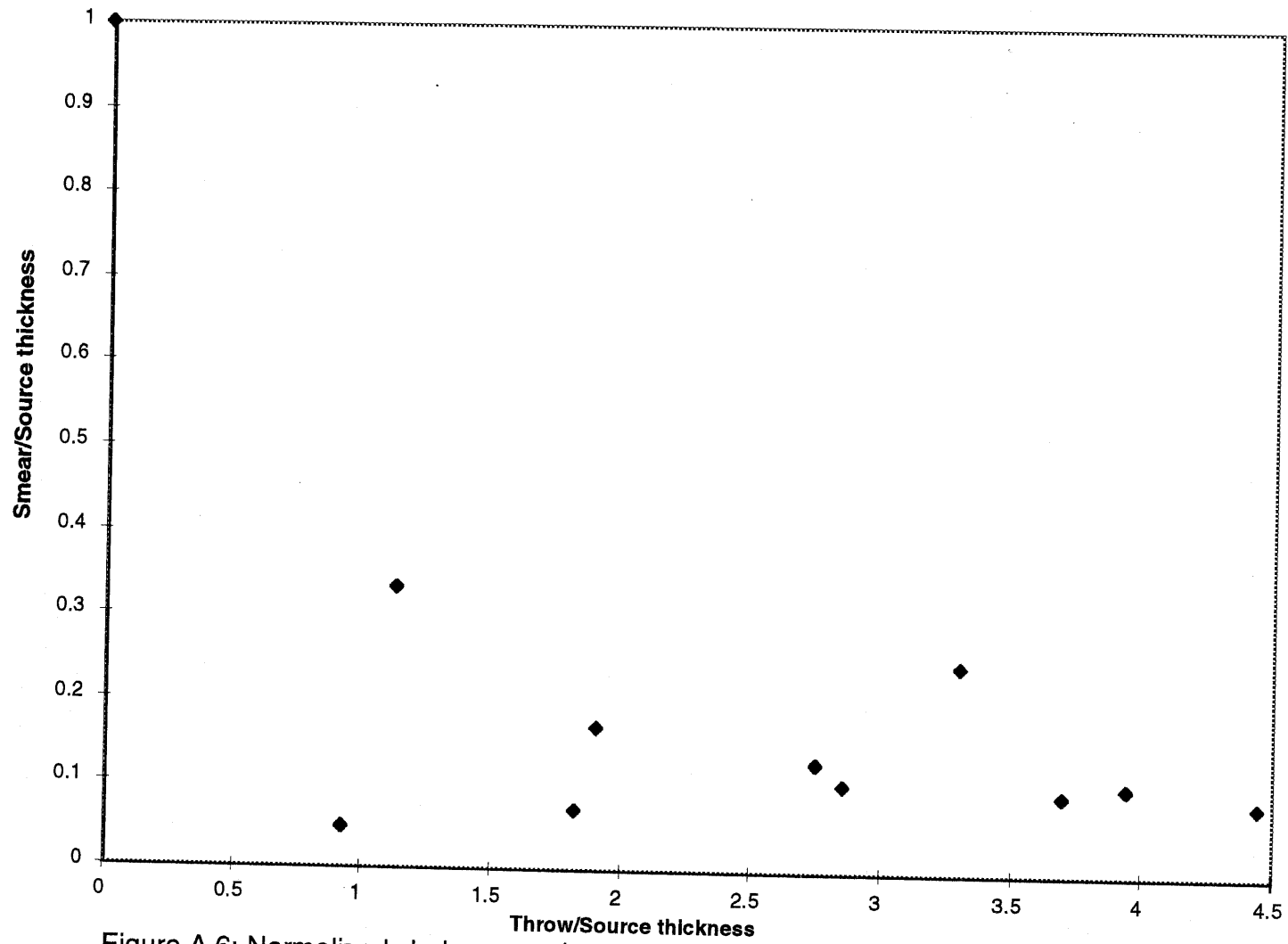


Figure A.6: Normalized shale smear (composite) vs. normalized fault throw.

References for Appendix A

Antonellini, M., and A. Aydin, 1994, Effect of faulting on fluid flow on porous sandstones: petrophysical properties: AAPG Bull. v. 78, p. 355-

Aydin, A. and Y. Eyal, Shale in fault zones and its effect on fault seal potential, Stanford Rock Fracture Project, v. 6,

Gibson, R. G., Fault_zone seals in siliciclastic strata of the Columbus Basin, Offshore Trinidad, AAPG Bull. v. 78, No 9, p. 1372-1385.

Koledoye, A. A., 1997, Methodology for analysing fault seal integrity in the Niger Delta, Stanford Rock Fracture Project, v 8, P. P-E-1 - P-E-9.

Lehner, F. K. and W. F. Pilaar, 1996, On a mechanism of clay smear emplacement in synsedimentary normal faults, In Norwegian Petroleum Society, eds., Hydrocarbon seals-Importance for Exploration and Production (conference abstracts) Norwegian Petroleum Society, Oslo. P.4.

Lindsay, N. G., Murphy, F. C., Walsh, J. J. and Watterson, J., 1993, Outcrop Studies of Shale smears on Fault Surfaces, Spec. Publs Int. Ass. Sediment Vol. 15, P. 113-123.

Tearpock, D. J. and Bishcke, R. E., 1991, Applied subsurface geological mapping, Englewood Cliffs, N. J., Prentice Hall.

Weber, K. J., Mandl, G., Pilaar, W. F., Lehner, F. and Precious, R. G. 1978, The role of faults in hydrocarbon migration and trapping in Nigerian growth fault structures: Offshore Technology Conference 10, paper OTC 3356, p.2643-2653.

Yielding, G., Freeman, B. and Needham, D. T., 1997, Quantitative fault seal prediction, AAPG Bull. V. 81, No. 6, P. 897-917

Younes, A. and A. Aydin, 1997, Relationship between fault offset and fault rock thickness: implications for fault seal potential, Stanford Rock Fracture Project, Vol. 8, P. B1-B10.



ES
04